Instrument Science Report STIS 2000-04

STIS Cycle 7 Calibration Close-out Report

Ilana Dashevsky and Melissa A. McGrath on behalf of the

Spectrographs Group: Jerry Kriss, Stefi Baum (ex officio), Ralph Bohlin (ex officio), Ron Downes, Linda Dressel, Brian Espey, Harry Ferguson (ex officio), Anne Gonnella, Paul Goudfrooij, Phil Hodge (Software Science Group), Jessica Kim, Howard Lanning, Claus Leitherer, Chris Long (Engineering Team), Rosa Diaz-Miller, Grace Mitchell, Charles Proffitt, Kailash Sahu, Ed Smith (ex officio), David Stys, Jeff Valenti, Nolan Walborn

STIS IDT: Bruce Woodgate, Ted Gull, Albert Boggess, Charles W. Bowers, Anthony Danks, Richard F. Green, Sara R. Heap, John B. Hutchings, Edward B. Jenkins, Charles L. Joseph, Mary Beth Kaiser, Randy Kimble, Steve Kraemer, Jeffrey L. Linsky, Stephen P. Maran, H. Warren Moos, Frederick Roesler, J. Gethyn Timothy, Donna E. Weistrop

August 1, 2000

ABSTRACT

The status and results of the Cycle 7 calibration program for the Space Telescope Imaging Spectrograph (STIS) are presented, based on more than two years of on-orbit calibration observations.

1. Introduction

The Space Telescope Imaging Spectrograph (STIS) was installed on the HST during the second Servicing Mission (SM2) in February 1997 (Woodgate *et al.* 1998). As a new instrument, the first Cycle (Cycle 7) of on-orbit calibration following the orbital verification program was extensive, involving over 80 calibration proposals executed over a 2.5 year time period. The calibration program measured the basic on-orbit performance of the instrument, provided on-orbit calibration for supported observing modes, and extended

measurements to modes not included in the ground calibration (Kimble *et al.* 1998, Ferguson 1998). The definition and oversight of this program was led by Harry Ferguson and Ed Smith.

The calibration program was developed in two stages: the CCD program was approved in March 1997, and the MAMA (multi-anode multiplexing array) program was approved in a *delta* to the initial program in February 1998. This was done in concert with the phased-in use of the MAMA detectors, which were not turned on until May 1997, months after the CCD began operation. The characteristics of the three detectors and their orientation with respect to the HST reference frame are given in Appendix A.

A grand total of 302 external and 2579 internal orbits were approved for the Cycle 7 calibration program. The overall status of the orbits is shown in Table 1. Several new calibration proposals were added after the review, subject to the approval of the TTRB, to address new issues or problems. An example is proposal 8056, which was added to help characterize the worsening CTE problem for STIS. A total of 300 external and 2748 internal orbits were executed. There were 16 external and 9 internal orbits that failed. Of these, 12 external and 1 internal orbits were repeated. Also, in the course of the Cycle, 47 external and 303 internal orbits were withdrawn following proposal implementation in favor of Cycle 8 and 9 calibration programs. (Proposal statistics courtesy of Nancy Fulton and Steve Dignan of the DDT.) The primary difference between allocated and executed internal orbits came from proposal 7783 (CCD sky parallels used for external flat-fields), which executed all observations not only in internal orbits, but in parallel, to maximize HST efficiency. Also, 3 internal contingency orbits were used for the NUV-MAMA anomalous recovery and fold distribution analysis. The NUV-MAMA safed when the Software Global Monitor event rate was exceeded on September 18, 1999. Subsequent analysis showed no degradation of the NUV-MAMA micro-channel plate (Long 1999a).

Table 1. Summary of orbit allocation and use during the Cycle 7 calibration of STIS.

Cycle 7 Orbits	External Orbits	Internal Orbits
Allocated	302	2579
Executed	300	2748
Withdrawn	47	303
Failed	16	9
Repeated	12	1

In addition to the execution and analysis of the calibration program, a routine program has been established to monitor the stability of STIS and proactively search for problems that could impact the quality of the data obtained. Seven areas are monitored, including: initial pointing stability, reference aperture stability, target acquisition accuracy, focus stability, MSM stability, lamp flux degradation, and long exposure pointing stability. The

monitoring program is described in detail in STIS TIR 98-07 (available only for STScI internal use).

The results of the Cycle 7 calibration proposals are summarized in Table 2. Details for each proposal are given on the page number listed in the last column. For ease of management of the calibration program, the proposals were divided into logical groups, such as CCD Monitoring, and each group of proposals had a Calibration Analysis Team (CAT) assigned responsibility for the data analysis and products. The proposals are therefore presented organized by their CAT group. For the Time Used (columns 3 and 4), we have summarized both the executed orbits, and the allocated orbits in square brackets [], on a proposal by proposal basis. To keep the size of the Phase 2 proposals manageable (for implementation purposes), particularly for the routine monitoring proposals (e.g., the CCD darks and biases), it was often necessary to split one particular aspect of the calibration into several separate Phase 2 proposals. While these were tracked separately, and are presented as separate proposals in the table, they are in fact a part of the same calibration and, for the sake of conciseness, are not treated as separate entities in the detailed forms following the table. The forms summarize the following five items:

1. Execution: success and frequency of proposal observations.
2. Summary of Goals: purpose of calibration.
3. Summary of Analysis: highlights of results and products, includes references for detailed analysis, procedures and/or requirements.
4. Accuracy Achieved: accuracy of the result or data processed using the calibration product.
5. Continuation Plans: follow-up calibration proposals or analysis.

Changing priorities and demands of the astronomy community influenced the course of the analysis and resulting products, which include some Cycle 8 calibration overlap. The primary products of the Cycle 7 calibration program were calibration reference files delivered to the OPUS Pipeline, STIS Instrument Science Reports (ISRs), STIS Technical Instrument Reports (TIRs), updates to the STIS Instrument Handbook (IHB), and articles presented at the 1997 HST Calibration Workshop, held at STScI in September 1997. Other products include the STIS Quick-Look Analysis Reports, which are only available from the STIS Internal Calibration Programs web site (*http://garnet.stsci.edu/STIS/html-internal/calibration/*), and the STIS IDT Post-Launch Quick-Look Analysis Reports available from the STIS IDT web site (*http://hires.gsfc.nasa.gov/stis/stispage.html*). The reference file products for individual proposals are identified by their suffix, listed in Appendix B. The STIS ISRs, TIRs, and IDT analysis reports are referenced by number (e.g., ISR 98-28). The author and date may be found from Appendix C. The STIS Quick-Look Analysis Reports and TIRs are available from the STIS Internal web site, which has restricted access.

The highlights of the Cycle 7 calibration program results include: changing several modes from available to supported, updated reference file sensitivities of all supported modes with on-orbit measurements, the development of the online STIS ETCs (Exposure Time Calculators) and the Target Acquisition Simulator, Synphot updates, IHB section on STIS data and calibration, updated dispersion solutions, production of on-orbit MAMA flat-fields, development of corrective techniques for CCD fringing, the routine production of weekly dark and bias reference files for the CCD, and numerous related IRAF scripts (available online from the HST Spectrographs web site *http://www.stsci.edu/instruments/stis)*.

The Cycle 7 results that led to modifications in future calibration programs include the scattered light in the echelle modes and worsening charge transfer efficiency. An algorithm was developed and implemented for removing the effects of scattered light in the echelle modes, which required resources from Cycles 8 and 9. The analysis to redo the echelle sensitivity measurements using the new correction algorithm is still ongoing. Degrading charge transfer efficiency in the CCD required the implementation of new calibration proposals. An example is the Cycle 8 proposal 8799, which was used to determine pseudo-aperture locations to improve the charge transfer efficiency by moving the default location from the center of the chip to a location closer to the read-out amplifier improving the charge transfer efficiency, especially for faint targets. Another example is the Cycle 9 proposal 8839, which measures the charge transfer efficiency for extended targets.

At the completion of this report, eight calibration proposals are still outstanding. In some cases, the analysis was combined with Cycle 8 calibration data or deferred to future Cycles. For almost all of these proposals the data has been used for the analysis of other calibration programs. The analysis is not critical and the outstanding Cycle 7 calibration issues may be summarized as:

1. non-standard sensitivity measurements (proposals 7917, 7937, 8066, and 8051),
2. prism and secondary wavelength settings sensitivity measurements (proposals 7809 and 7810), and
3. full-field sensitivity measurements (proposals 7639 and 7720).

The Cycle 7 STIS calibration program was a monumental achievement. The dedicated efforts of many people not listed on this report went into making it a success. Although it would be virtually impossible to mention everyone by name, we acknowledge here our sincere gratitude for their efforts.

Table 2. STIS Cycle 7 Calibration Closure Summary

ID	Proposal Title	Time Used (orbits) *executed [allocated]*		Products	Accuracy Achieved	Page
		External	Internal			
CCD Monitoring and Detector Calibration						
7600	CCD Performance Monitor		25 [25]	ISR 98-31; Kimble *et al.* 1998; drk and bia reference files; STIS Flight Software updates.	Bias level: 0.1 ADU and dark current: 0.5 e^- /hr, which has *rms* noise level: 0.05 e^- /hr/pixel.	page 11
7601	CCD Dark and Bias Monitor		182 [182]	ISR 99-08; drk, bpx, bia reference files; scripts for creating darks available online.	Accuracy of the gain: 1-3% and read-out noise: 2-3%, depending on binning.	page 13
7602	CCD Flat Field Programme		6 [2]	ISR 99-06; Kaiser *et al.* 1998; pfl reference files.	Flat-field *rms*: < 0.1% for the low or medium dispersion average flat.	page 16
7634	CCD Flat-Field Stability and Cosmetic Defect Fraction		15 [16]	ISR 99-04; Ferguson 1997; pfl reference files	Flat-field *rms*: ~0.3% and temporal variation: < 1%/year.	page 15
7635	CCD Hot Pixel Annealing		77 [114]	ISR 98-06; Beck *et al.* 1997; Hill *et al.* 1997.	Monthly anneals anneal out (80 ± 5)% of hot pixels.	page 20
7636	Spectroscopic CCD Flat Fielding		9 [9]	See proposal 7602.	See proposal 7602.	page 16
7637	CCD Residual Images after Saturation	4 [4]		IHB, ch. 7 update.	Not available.	page 19
7659	Daily Darks to Update Acquisition Bad Pixel Table		109 [112]	TIR 98-05; scripts for creating darks available online.	S/N: 5-10 σ above median dark current.	page 14
7711	CCD G750L Fringing Flats		45 [45]	ISRs 99-06, 98-29, 98-19; Goudfrooij *et al.* 1997; IHB, ch. 7 update; scripts available online for fringe flats.	G750L mode flat: reduce fringe residuals with the 1% level.	page 17
7783	CCD External Flats, Sky Parallels		504 [150]	Reference file: jaj1058ho_lfl.	Corrects 5-10% sensitivity roll off within about 60 pixels from the edge of the 50CCD aperture.	page 18
7802	Daily Darks to Update Acquisition Bad Pixel Table		103 [103]	See proposal 7659.	See proposal 7659.	page 14
7803	Daily Darks to Update Acquisition Bad Pixel Table Part III		110 [112]	See proposal 7659.	See proposal 7659.	page 14
7926	CCD Dark and Bias Monitor -- Continued		129 [182]	See proposal 7601.	See proposal 7601.	page 13

7928	Spectroscopic CCD Flat Fielding -- Continued		9 [17]	See proposal 7602.	See proposal 7602.	page 16
7930	CCD Binned Bias Monitor		6 [6]	ISR 98-31; bia reference files.	S/N = 4 per pixel for 1x2 binning.	page 14
7944	Sparse Field CTE Test	0 [2]	22 [48]	See proposal 7600.	See proposal 7600.	page 11
7948	CCD Dark and Bias Monitor -- Continued to Dec. ‘98		506 [476]	See proposal 7659.	See proposal 7659.	page 14
7949	CCD Dark and Bias Monitor -- Continued to Jun. ‘99		178 [336]	See proposal 7601.	See proposal 7601.	page 13, page 14
7969	CCD G750L Fringe Flats at Intermediate MSM positions		10 [0]	See proposal 7711.	See proposal 7711.	page 17
8056	External Sparse Field CTE Test	2 [0]		IHB, ch. 7 update; Goudfrooij 2000; Gilliland *et al.* 1999.	CTE performance loss of 1% for signal levels of 100-200 electrons at the center of the chip.	page 21
8057	CCD Performance Monitor (continued)		51 [0]	See proposal 7600.	See proposal 7600.	page 11
8080	Spectroscopic CCD Flat Fielding -- Revised		38 [0]	See proposal 7602.	See proposal 7602.	page 16
8081	CCD Hot Pixel Annealing -- II		39 [0]	See proposal 7635.	See proposal 7635.	page 20
MAMA Monitoring and Detector Calibration						
7604	Cycle 7 MAMA Dark Measurements		254 [257]	ISR 99-02; IHB, ch. 7 update; drk reference files.	FUV-MAMA: ~7 cts/sec and NUV-MAMA: 800-2000 cts/sec.	page 22
7644	NUV-MAMA Monitoring Flats		7 [7]	ISR 98-15; Kaiser *et al.* 1998 pfl reference files.	1% accuracy per pixel.	page 23
7645	FUV-MAMA Cycle 7 Flats		23 [40]	Ferguson 1998, Kaiser *et al.* 1998; reference file: ibn1813ro_pfl.	Evidence for variation at the 1 to 2 % per year per resolution element.	page 24
7647	NUV-MAMA Cycle 7 Flats		20 [40]	Ferguson 1998, Kaiser *et al.* 1998; reference file: ibn18109o_pfl.	See proposal 7645.	page 24
7670	MAMA Ramp-up Check	2 [4]		STIS Quick-Look Report 7670.	Target not properly acquired.	page 25
7728	FUV-MAMA Monitoring Flats		8 [8]	See proposal 7644.	2% per low-resolution pixel.	page 23
7937	MAMA Off Axis Sensitivity (Vignetting)	4 [4]		ISR in progress (N. Walborn).	Not available.	page 25
7950	Cycle 7 MAMA Dark Measurements		165 [158]	See proposal 7604.	See proposal 7604.	page 22
7965	MAMA Fold Analysis for Cycle 7		4 [0]	STIS Engineering Update 99:195.	No degradation: deviation of less than 20% relative to past results.	page 26
Spectroscopic Wavelength and Geometric Distortion						

7648	CCD G230LB and G230MB Wavelength Calibrations		2 [2]	ISR 98-23; STIS Quick-Look Report 7648; reference file: j1c1746jo_dsp.	Calculated and measured dispersions agree with the measurements to within ~0.1%.	page 27
7649	MAMA Missed Dispersion Solutions		6 [6]	IDT Quick-Look Report 062; dsp reference files.	*Rms* values range from 0.16 to 0.27 (STIS Quick-Look Report 7649).	page 27
7650	Yearly CCD Wavelength Monitor		8 [12]	ISR 98-23; reference file: j1c1746jo_dsp.	Dispersions agree with the measurements to within ~0.1%.	page 28
7651	MAMA Dispersion Solution Check		20 [24]	1st-order did not need update; dsp reference file update in progress.	1st-order observing modes did not need update; echelle modes: see proposal 7649.	page 28
7652	LSF Measure of the CCD-Spectroscopic Modes	3 [3]		ISR 98-04; IHB, ch. 13.	FWHM uncertainty: 2 0.2 pixels FWHM *rms*:~2-3%.	page 29
7653	LSF Measure of the CCD-Spectroscopic Modes	4 [3]		See proposal 7652.	See proposal 7652.	page 29
7654	Slitless Spectroscopy, CCD	4 [4]		IHB, ch. 12 update.	Not available.	page 30
7665	CCD Geometric Distortion CCD	2 [4]		TIR in progress (B. Espey); IHB, ch. 14 update; sdc reference file update in progress.	Agreement between WFPC-2 PC and STIS images agree to 0.5 pixels across the chip, distortions < 1 pixel across the detector.	page 31
7667	MAMA Geometric Distortion	5 [5]		See proposal 7665.	Distortions are larger than for CCD and vary, approaching 3 pixels at the corners of the cameras.	page 31
7668	Incidence Angle Correction for Non-Concentric Slits-CCD		4 [8]	Iac reference file, based on model data, does not require update.	Not available.	page 32
7669	Incidence Angle Correction for Non-Concentric Slits-MAMA		18 [38]	Iac reference file update in progress.	Not available.	page 33
7936	External to Internal Wavelength Correction Calibration	3 [3]		ISR 99-01.	Line centers: within 0.1 pixels or 0.27 Å for G430Land 0.06 Å for G750L modes, emission lines: < 8 km/sec FWHM.	page 34
Spectroscopic Photometry						
7656	Spectroscopic and Imaging Sensitivity, CCD	19 [27]		ISR 99-07; IHB, ch.'s 5, 14, and 16 updates; pht reference files.	Spectroscopic accuracy: 2-5%, imaging accuracy: 5%.	page 35
7657	Spectroscopic and Imaging Sensitivity, MAMA	54 [72]		See proposal 7656.	Spectroscopic accuracy: 2-8%, imaging accuracy: 5%.	page 35
7672	CCD Sensitivity Monitor	18 [18]		ISRs 99-07, 99-04, 98-2; pht reference files.	Photometric precision for the 52x2 slit given in Table 8.	page 37

7673	MAMA Sensitivity and Focus Monitor	43 [42]		ISRs 99-07, 98-20, 98-09, 98-01; pht reference files.	Photometric precision for the 52x2 slit given in Table 8, for the echelle modes (using 0.2x0.2 slit) refer to Table 9.	page 37
7674	IR Standards	27 [0]		Bohlin 2000.	Residuals with respect to the LTE model continua are less than ~1% from 2000 to 9000 Å.	page 41
7723	Grating scatter	4 [4]		STIS Quick-Look Report 7723.	Not available.	page 39
7805	Contamination: Tie SMOV Stars to Cycle 7 Star	3 [3]		ISRs 98-20, 98-27; Bohlin 2000.	See proposal 7674.	page 40
7809	Prism Sensitivity and Faint Calibration Standard Extension	1 [3]		Analysis is deferred to Cycle 9.	Not available.	page 41
7810	Sensitivity of Important Secondary Wavelength Settings	1 [2]		Analysis is deferred to Cycle 9.	Not available.	page 42
7917	Effect of MAMA Charge Offsetting on Sensitivity and Dispersion Accuracy	2 [4]		Analysis in progress.	Not available.	page 42
7931	Scattered light in the Echelle Modes	6 [13]		The STIS IDT algorithm for echelle scatter correction (Quick-look Analysis Report 059) has been implemented as an option, called *sc2d*, in the IRAF STIS package X1D task for spectral extraction.	Preliminary analysis shows that the mean flux corrected for scattered light has an accuracy between 0.05% to 1.9% and the change in flux using the 2-D correction relative to the 1-D is between -0.1% to 4.9%, depending on the echelle mode.	page 43
7932	Spectral Purity and Slit Throughputs for the First Order Spectroscopic Modes	11 [11]		ISRs 98-27, 98-20; IHB, ch. 13 update.	CCD throughputs are accurate to within 10%.	page 44
7943	Transmission of Filtered Echelle Slits	2 [2]		ISR 98-25, IHB, ch. 13 update.	Not available.	page 45
8016	Effect of MAMA Charge Offsetting on Sensitivity and Dispersion Accuracy - Repeat	4 [0]		Analysis in progress.	Not available.	page 42
8066	IR Standards: HZ43 Repeat	4 [0]		Bohlin 2000.	See proposal 7674.	page 41
8067	Improved STIS Sensitivity Measurement for E140H	3 [0]		Analysis ongoing with 2-D scatter correction (see proposal 7931).	The accuracy of the mean flux in the core of saturated interstellar lines is 0.4% at 1200 Å and 0.1% at 1670 Å, with the scattered light correction.	page 46
Imaging Photometry and Geometry						
7639	CCD Imaging Sensitivity Monitor (over full-field)	5 [7]		Analysis in progress.	Not available.	page 47

7641	CCD External Flats, Stellar	2 [2]		STIS Quick-Look Report 7641 Ferguson *et al.* 1997.	Using the pipeline flats, relative photometry looks good to better than 0.02 magnitude.	page 47
7642	CCD Red Light PSF Halo	2 [2]		STIS Quick-Look Report 7642 further analysis is in progress (C. Proffitt).	F28X50LP images: 80% of the total flux in an aperture of radius of 3 pixels; OIII images: 80% of the energy is encircled in a 4 pixel aperture.	page 48
7661	MAMA Filter Red Leak Measurement	4 [4]		STIS Quick-Look Report 7661 IDT Quick-look Reports 023, 016, 008, reference file update for F25SRF2 filter: j781536qo_apt.	Measurements agree within 3-5% with previous throughputs.	page 49
7666	CCD Linearity and Shutter Stability	3 [3]	4 [4]	ISR 99-05, Gilliland *et al.* 1999.	See Gilliland *et al.* 1999.	page 50
7720	MAMA Full Field Sensitivity Monitor and PSF Check	10 [10]		Analysis in progress.	Throughputs good to within 5%.	page 51
7774	Deep MAMA PSFs	3 [3]		Apt reference files; PSF database in progress; IHB, ch.'s 7 and 14 updates.	Fraction of flux enclosed within a 0.05 arcsec radius aperture varies across detector.	page 52
7788	MAMA Image Location and Geometric Distortion	3 [3]		IHB, ch. 14 update; Malumuth & Bowers 1997.	Plate scale accuracies better than 0.1%.	page 53
8069	Throughput of F25ND5 Filter	2 [0]		ISR in progress (C. Proffitt); reference file: j781536qo_apt; Synphot & IHB, ch. 14 updates.	Imaging throughputs are within 30% of the pre-launch estimates.	page 54
8070	Throughput of NUV Filters	2 [0]		ISR in progress (C. Proffitt); STIS Quick-Look Report 7661; reference file: j781536qo_apt; Synphot & IHB, ch. 14 updates.	FUV-MAMA imaging: within 6% of the pre-launch estimates and NUV-MAMA imaging: within 2% to 17% of pre-launch predictions.	page 55
8438	CCD Saturated Photometry	1 [0]		ISR 99-05.	Time series S/N of about 10000 per readout demonstrated.	page 56
Operations and Engineering						
7605	CCD Target Acquisition Workout	6 [6]		TIR 99-04; IHB ch. 8.	Point source: 0.01 arcsec and diffuse source: 0.01-0.1 arcsec.	page 57
7643	MAMA Fold Analysis for the Anomalous Recovery Procedure		1 [6]	STIS Technical Report 99:287 (draft).	No degradation: measurements within 20% of past results.	page 58
7646	CCD Scattered Light Near Earth Limb	8 [8]		ISR 98-21.	Background of the scattered light from the Earth limb measured to 0.001 e^-/sec/pix.	page 59

7660	STIS to FGS Alignment Check	1 [1]	2 [2]	PDB SIAF file update.	Aperture position zero point: 0.1 arcsec and rotation angle: < 0.5 degrees.	page 57
7719	FUV MAMA Anomalous Recovery Procedure	[0]	[0]	Not applicable.	Not applicable.	page 60
7721	Slit Throughputs	5 [5]		ISRs 98-20, 98-01; apt reference files.	1 σ scatter (*rms*): ~1-12% depending on aperture for MAMA.	page 61
7722	Lamp Flux Measurement		25 [25]	TIR 98-07; STIS Flight Software table update; ETC update.	Not applicable.	page 62
7725	NUV MAMA Anomalous Recovery Procedure		2 [0]	STIS Technical Report 99:287.	Not applicable.	page 60
7905	CCD Acquisition Checkout Flight Software Hot Pixel Fix	4 [4]		STIS Flight Software update; STIS Quick-Look Report 7905.	Accuracy of acquisitions for point source: 0.1 pixels, diffuse source: 1.1 and 1.4 pixels, and point source (ACQ/PEAKs): 0.05 pixels (3% of the aperture size).	page 63
7951	Anomalous Scatter Calibration	1 [3]		CCD observations include the occulting bar (52X0.2F1); analysis may be out sourced.	Not available.	page 63
7953	Slit Wheel Repeatability		1 [1]	STIS Quick-Look Report 7953.	0.01 pixels or 0.5 milli-arcsec.	page 64
8051	Out-of Focus PSF	3 [0]		Analysis in progress.	Not available.	page 65
8397	MSM Update Spectroscopic Verification		1 [0]	MSM update was successful.	FUV-MAMA plate scale accuracy is 0.08%.	page 65
Withdrawn or Replaced						
7934	Repeller Wire Off Test	0 [1]	0 [2]	Replaced with Cycle 8 calibration proposal 8431.	Observations were withdrawn.	page 66
7935	Cross Disperser Mode Test	0 [3]	0 [2]	Withdrawn due to lack of GO interest; TIR 97-22.	Observations were withdrawn.	page 66
7942	MSM Update, Test		0 [2]	See proposal 8397.	Replaced with proposal 8397.	page 66
TOTAL ORBITS EXECUTED Number of Allocated Orbits		**300 [302]**	**2748 [2579]**			

2. CCD Monitoring and Detector Calibration

Proposal IDs 7600, 7944, 8057: CCD Performance Monitor

Execution	The frequency of the observations is every 6 months. Executed as planned on Jun., Aug., Sept., Dec. 1997, and on Jun., Nov. 1998, as well as, May 1999.
Summary of Goals	Measure the baseline performance of the CCD. Baseline performance from the SM2 SMOV given in ISR 97-10.
Summary of Analysis	The analysis is given in the ISR 98-31 and Kimble *et al.* 1998, see Fig. 1. The products include reference file updates (drk, bia), flight software updates of tables *CCDBiasSubtractionValue*, *BadPixelTable*, and *NumBadPixels*, read noise and gain measurements listed in Table 3 and Table 4.
Accuracy Achieved	Bias level: better than 0.1 ADU at any position within CCD frame, the read-out noise negligible. Dark current: good to 0.5 electron/hour, the *rms* noise level is about 0.05 electron per hour per pixel. The systematic error in hot pixels may well exceed this limit.
Continuation Plans	Continued with Cycle 8 CCD Performance Monitor proposal 8407.

Figure 1: Portion of an unbinned superbias frame shows a “ripple” pattern (due to electronic pick-up noise) of an image taken in CCDGAIN=4, which is not removed by biases. This effect is not evident in CCDGAIN=1 images (ISR 98-31).

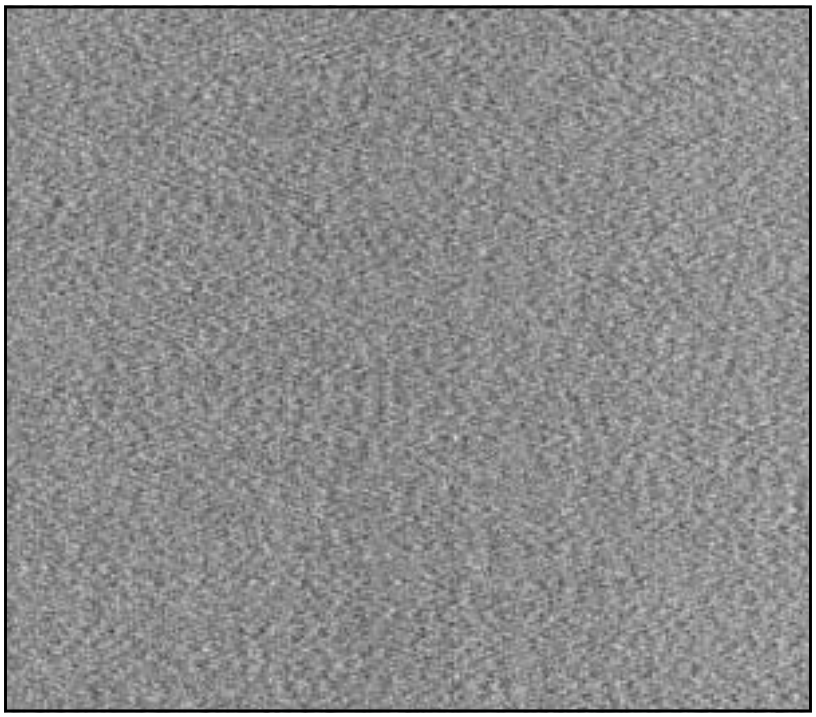

The following tables from the ISR 98-31 summarize the CCD gain and read-out noise measurements during Cycle 7. These values are consistent with the pre-launch measurements, except for the read-out in the high gain settings (2, 4, 8), which is higher in orbit. This is due to electronic pick-up pattern noise (Fig. 1), which raises the effective read-out noise.

Table 3. CCD Gain values, measured in electrons/DN, as a function of time.

Gain Setting	Bin Size	Pre-launch Gain	Gain Mar. 1997	Gain Jun. 1997	Gain Dec. 1997	Gain Jun. 1998	Gain July 1998
1	1x1	0.994 0.008	0.97 ± 0.02	0.98 ± 0.02	0.99 ± 0.02	1.00 ± 0.02	1.00 ± 0.02
1	1x2	0.995 ± 0.005	0.98 ± 0.02	0.96 ± 0.02	0.99 ± 0.02	1.01 ± 0.02	1.01 ± 0.02
1	2x1	0.995 ± 0.013	1.00 ± 0.01	1.01 ± 0.02	1.03 ± 0.02	0.99 ± 0.02	0.99 ± 0.01
1	2x2	1.001 ± 0.010	1.00 ± 0.01	1.00 ± 0.02	1.01 ± 0.03	1.00 ± 0.02	1.00 ± 0.01
	4x1	0.984 ± 0.024	~	0.96 ± 0.03	0.97 ± 0.03	0.99 ± 0.03	0.99 ± 0.03
1	4x2	1.008 ± 0.013	~	~	0.97 ± 0.03	1.01 ± 0.03	1.01± 0.03
2	1x1	2.008 ± 0.006	2.00 ± 03	2.01 ± 0.02	~	2.02 ± 0.02	2.02 ± 0.02
4	1x1	4.069 ± 0.009	~	4.00 ± 0.05	4.07 ± 0.05	4.08 ± 0.05	4.08 ± 0.05
8	1x1	8.323 ± 0.027	~	8.07 ± 0.10	~	8.05 ± 0.10	8.05 ± 0.10

Table 4. CCD read noise values, measured in electrons, as a function of time.

Gain Setting	Bin Size	Pre-launch Read Noise	Read Noise Mar. 1997	Read Noise Jun. 1997	Read Noise Dec. 1997	Read Noise Jun. 1998	Read Noise July 1998
1	1x1	4.0	3.78 ± 0.05	3.98 ± 0.06	3.95 ± 0.08	4.02 ± 0.08	4.02 ± 0.08
1	1x2	~	4.18 ± 0.05	3.83 ± 0.08	3.99 ± 0.09	4.05 ± 0.11	4.05 ± 0.11
1	2x1	~	3.65 ± 0.03	3.70 ± 0.09	3.87 ± 0.07	3.69 ± 0.09	3.69 ± 0.09
1	2x2	~	3.76 ± 0.03	3.70 ± 0.12	3.85 ± 0.15	3.85 ± 0.10	3.85 ± 0.10
	4x1	~	~	3.69 ± 0.13	3.59 ± 0.10	3.73 ± 0.12	3.73 ± 0.12
1	4x2	~	~	~	3.66 ± 0.09	3.84 ± 0.20	3.84 ± 0.20
2	1x1	4.8	5.32 ± 0.10	5.75 ± 0.10	~	5.79 ± 0.12	5.79 ± 0.12
4	1x1	6.4	~	7.50 ± 0.21	7.22 ± 0.11	7.65 ± 0.16	7.65 ± 0.16
8	1x1	10.4	~	11.87 ± 0.21	~	12.24 ± 0.30	12.24 ± 0.30

Proposal IDs 7601, 7926, 7948, 7949: CCD Dark and Bias Monitor

Execution	Proposals 7601 and 7926 executed 7 times per week each, and proposals 7948,7949 executed 14 times per week each.
Summary of Goals	Monitor and update the darks and biases for the CCD. Refer to the TIR 98-05 for details on CCD dark frame procedures.
Summary of Analysis	The analysis for CCD biases described in the ISR 99-08. Also, refer to Fig. 2 and Table 5. Products from the monitors include reference file updates (drk, bpx, bia, superbias every 6 months, weekly bias and superbias for hot column removal), read noise and gain measurements.
Accuracy Achieved	The gain is measured to an accuracy of 1-3% and read-out noise is measured to an accuracy of 2-3%, depending on binning.
Continuation Plans	The bias frame frequency increased in Cycle 8 due to insufficient S/N per pixel (Table 5) for weekly superbiases. Darks and biases in separate proposals: 8408, 8437 for the darks and 8409, 8439 for the biases.

Figure 2: Left: grey scale comparison of superbias frames taken in CCDGAIN=1 from Sept. to Nov. 1997 (top left) with one taken during July 1999 (bottom left). **Right:** Comparison of a sparse star field using a weekly dark reference file (top right) and using both weekly bias and dark reference files (bottom right). Notice the significant improvement in cosmetic appearance. (ISR 99-08)

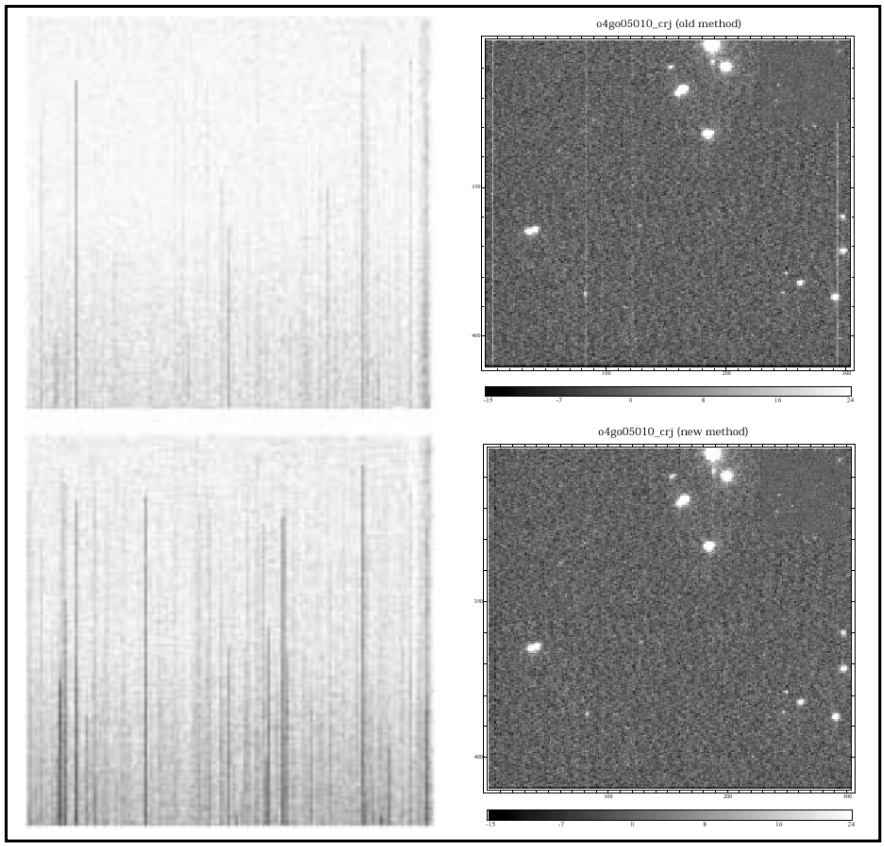

Proposal IDs 7659, 7802, 7803, 7948, 7949: CCD Daily Darks

Execution	Once a day for CCDGAIN=4 and twice a day for CCDGAIN=1.
Summary of Goals	Monitor and update the CCD daily dark reference files. The daily darks are used to identify hot pixels.
Summary of Analysis	The analysis resulted in weekly reference file updates (drk) and flight software updates. Refer to the TIR 98-05 for a description of daily dark creation. IRAF scripts available online for use in creating daily darks.
Accuracy Achieved	For daily darks taken 2 days prior to science observations a S/N of 5-10 σ above the median dark current may be achieved.
Continuation Plans	Daily darks are taken as part of proposals 8408 and 8437.

Proposal ID 7930: CCD Biases for 1x2 Binning

Execution	30 biases taken every three months.
Summary of Goals	Measure read noise and gain for 1x2 binned biases.
Summary of Analysis	The analysis is described in the ISR 98-31. Refer to the ISR 99-08 for CCD bias creation and testing procedure (see Table 5). Results given in Table 3 and Table 4. Products include reference file updates (bia).
Accuracy Achieved	S/N = 4 per pixel was achieved with Cycle 7 biases, using 1x2 binning.
Continuation Plans	Continued in the CCD Bias Monitor proposals 8409 and 8439. Bias frame frequency increased for sufficient S/N per pixel.

Table 5. The number of STIS CCD bias frames to be combined together in order to obtain S/N = 1 per pixel for superbias images taken in all the supported gain and binning settings (ISR 99-08).

CCDGAIN Setting	Binning	Read-out Noise Per Pixel (ADU)	Median Intensity Level in Bias Frame (ADU)	Number of Frames for S/N=1 Per Pixel
1	1x1	4.0	0.40	100
1	1x2	4.0	0.64	39
1	2x1	4.0	0.65	38
1	2x2	4.0	1.19	11
1	4x1	4.0	1.19	11
1	4x2	4.0	1.86	5
4	1x1	1.89	1.45	2

Proposal ID 7634: CCD Flat Field Monitoring

Execution	Executed monthly.
Summary of Goals	Investigate flat-field stability over a monthly period. Technical requirements for flat-fielding are discussed in the TIR 97-16.
Summary of Analysis	The analysis is described in the ISR 99-04 and Ferguson 1997, (see Fig. 3). The products include reference file updates (pfl) for the 50CCD and F28X50LP imaging flats.
Accuracy Achieved	Application of a flat-field to spectra of standard stars produces an *rms* residual noise level as good as ~0.3%, which is comparable to the residual noise achievable with no flat-fielding. The CCD flat-fields have a temporal variation of < 1% per year.
Continuation Plans	Continued in the Cycle 8 proposal 8412, including the F28X50OII and F28X50OIII filters.

Figure 3: The CCD flat-field (low resolution mode) shows dust mote features, which are shadows of specks of dust on the CCD window and blemishes. The medium resolution flat-field has larger and shallower dust motes. Since flat-field correction of the dust motes is inadequate for spectra of point sources, these artifacts can be up to 3% deep with a width of several pixels after flat-field correction. (ISR 99-04)

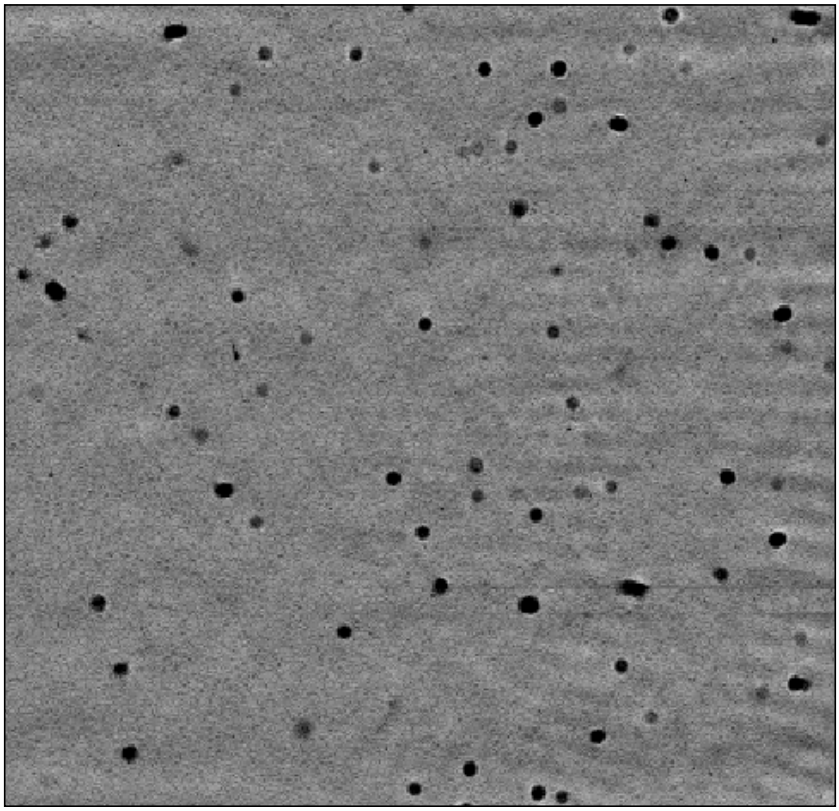

Proposal ID 7602: Missing CCD Flats (Spectroscopic)

Execution	Executed twice during Feb. and Mar. 1998.
Summary of Goals	Obtain flats for the G230LB and G230MB observing modes. Technical requirements given in the TIR 97-16.
Summary of Analysis	The analysis is given in the ISR 99-06 and Kaiser *et al.* 1998. Products include reference files (pfl) for the missing observing modes.
Accuracy Achieved	Refer to Table 6.
Continuation Plans	Continued in Cycle 8 as part of proposal 8411.

Proposal IDs 7636, 7928, 8080: CCD Spectroscopic Flats

Execution	Executed monthly.
Summary of Goals	Obtain flat-fields for the CCD spectroscopic observing modes. Technical requirements in TIR 97-16.
Summary of Analysis	The analysis is described in the ISR 99-06 and Kaiser *et al.* 1998. Products include reference file updates (pfl).
Accuracy Achieved	Refer to Table 6.
Continuation Plans	Continued in Cycle 8 as part of proposal 8411.

Table 6. The intrinsic *rms* fluctuation in the CCD flat-field is 0.8%, thus flats that have less than 0.8% statistical significance produce spectra that are always noisier than with no flat. The PGCCDL and PGC-CDM, low and medium dispersion respectively, averaged flats are recommended. (ISR 99-06)

Mode	rms (%)	Mode	rms (%)	Mode	rms (%)	Mode	rms (%)
PGCCDL, PGCCDM	**0.066**	**G230LB**	2375 Å: 0.72	**G430L**	4300 Å: 0.26	**G750L**	7751 Å: none

Mode	rms (%)	rms (%)	rms (%)	rms (%)	rms (%)	rms (%)	rms (%)
G230MB	1713, 1854, 1995 Å: none	2135 Å: 0.79	2276 Å: 0.44	2416 Å: 0.90	2557 Å: 0.58	2697 Å: 1.23	2836 Å: 0.80
	2976 Å: 0.55	3115 Å: 0.65					
G430M	3165 Å: 0.38	3423 Å: 0.56	3680 Å: 0.76	3936 Å: 0.48	4194 Å: 1.21	4451 Å: 1.01	4706 Å: 0.82
	4961 Å: 0.57	5261 Å: 0.62	5471 Å: 0.61				
G750M	5734 Å: 0.31	6252 Å: 0.36	6768 Å: 0.39	7283 Å: 0.36	7795 Å: 0.37	8311 Å: 0.40	8825 Å: 0.35
	9336 Å: 0.32	9851 Å: 0.35	10,363 Å: 0.63				

Proposal IDs 7711, 7969: CCD Fringe Flats

Execution	Proposal 7711 executed bi-weekly from Oct. 1997 to Mar. 1998, proposal 7969 executed between July 27 and 29, 1998.
Summary of Goals	Investigate and monitor the CCD flat-field fringing in the G750L observing mode at the central wavelength 7751 Å.
Summary of Analysis	The analysis is discussed in the ISRs 99-06, 98-29, 98-19, Goudfrooij *et al.* 1997, and the IHB, ch. 7. Also, refer to Fig. 4. Preliminary analysis is given in the TIRs 97-16, 97-15, and Plait & Bohlin 1997. IRAF scripts available online or in the STIS package for creating contemporaneous fringe flats.
Accuracy Achieved	For G750L long-slit spectra, a contemporaneous tungsten flat field can reduce fringe residuals below the 1% level, for point sources (flat taken with the small slit) and extended objects.
Continuation Plans	Not continued in Cycle 8. Contemporaneous flats should be requested by the General Observer for best results.

Figure 4: Top left: the CCD fringe flat for the G750L grating. **Bottom left:** the CCD fringe flat for the G750M grating (not included in proposals 7711 and 7969). The fringes are caused by interference of multiple reflections between two surfaces of the CCD, evident only in the G750 modes for STIS. (ISR 98-19) **Right:** Comparison of de-fringing capabilities of pipeline flats and those of contemporaneous (taken during science observations) flats. (IHB, Fig. 7.1).

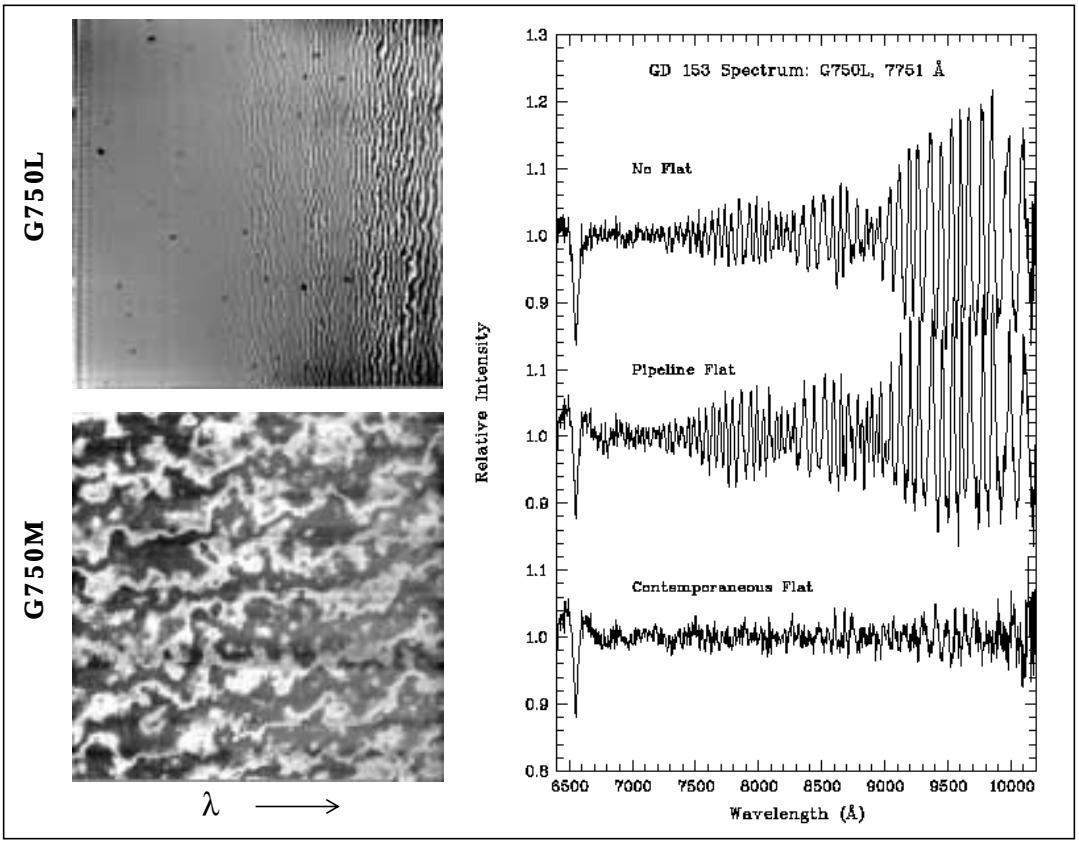

Proposal ID 7783: CCD External Flats

Execution	Several times a month between Aug. 1997 and Jan. 1998. Approved 150 external orbits extended to 504 non-proprietary, parallel orbits, at no fixed pointing, 400 seconds per exposure.
Summary of Goals	Obtain an independent measurement of the spatial sensitivity variations of the CCD using sky flats. Also, test the applicability of internal flats to astronomical sources. Requirements discussed in the ISR 96-15.
Summary of Analysis	Data from proposal 7783 was used for the preliminary analysis, however, the final reference file was made from the Hubble Deep Field South (HDF-S), proposal 8071, for STIS imaging. Products include the improved CCD low-order flat reference file (jaj1058ho_lfl), see Fig. 5, and the HDF-S low-order flat-field (Gardner *et al.* 2000).
Accuracy Achieved	Corrects 5-10% sensitivity roll-off within about 60 pixels from the edge of the 50CCD aperture.
Continuation Plans	There is no Cycle 8 continuation plan.

Figure 5: A Low-order flat-field image created using HDF-S flanking field images from proposal 8071 (reference file jaj1058ho_lfl). The image is displayed using a logarithmic stretch, with the grey scale: contrast=5.0 and brightness=0.94.

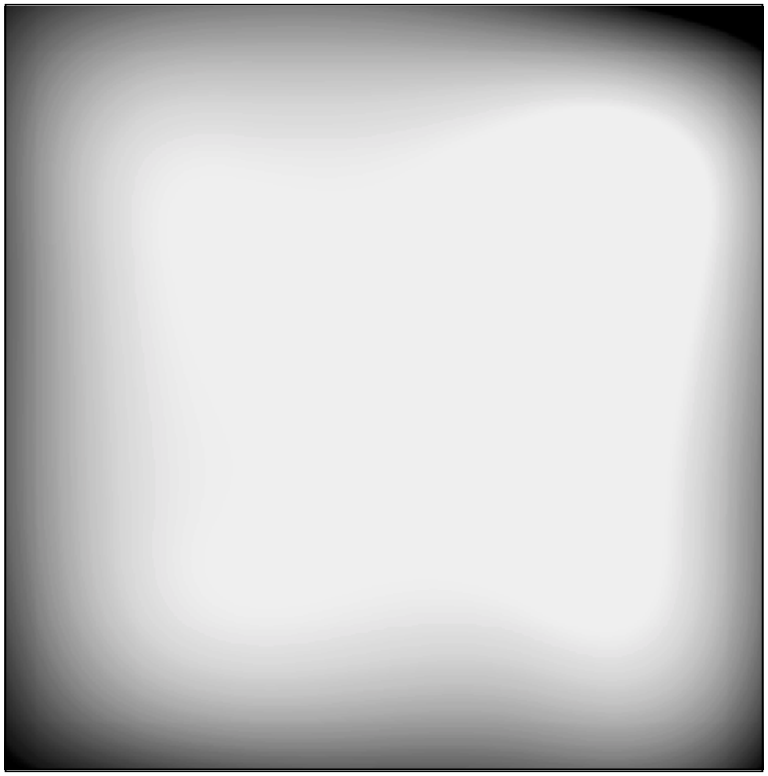

Proposal ID 7637: CCD Residual Images Following Over Illumination

Execution	Executed on Oct. 6-7, 1997.
Summary of Goals	Measure the residual effect of over illumination of the CCD as a function of color (UV and RED).
Summary of Analysis	A residual effect was not apparent (P. Goudfrooij private communication). The analysis from ground testing is given in Table 7. More discussion in the IHB, ch. 7.
Accuracy Achieved	Not available.
Continuation Plans	Re-measure in Cycle 9 (proposal 8853) to determine the effect of charge transfer inefficiency on residual images following over illumination.

Table 7. Effect of CCD UV over illumination on elevation of dark current, based on ground testing (IHB, Table 7.6).

Over illumination Rate (e^- $pixel^{-1}$)	Initial Dark Current Elevation (%)	Time to Return to Nominal
500,000	500	30 min
5,000,000	1500	40 min

Proposal IDs 7635, 8081: CCD Hot Pixel Annealing

Execution	Executed monthly starting July 1997 (2 orbits failed).
Summary of Goals	Monitor the flat-field stability over a monthly period.
Summary of Analysis	The analysis is given in the ISR 98-06 (see Fig. 6). Also, refer to Beck *et al.* 1997 and Hill *et al.* 1997.
Accuracy Achieved	Monthly anneals anneal out (80 ± 5)% of hot pixels (hotter than 0.1 e^- sec^{-1} pix^{-1}), which grow at a rate of 0.5 per day *between* CCD anneals.
Continuation Plans	Continued during Cycle 8 in calibration proposal 8410.

Figure 6: Plot of hot pixels (caused by radiation damage) in the STIS CCD as a function of time. The vertical lines represent a monthly anneal, when the CCD is increased to ambient temperature from its normal operating temperature of -83˚C. The total number of hot (> 0.1 e^- sec^{-1} pix^{-1}) pixels is ~10,000 after an anneal (March 1999). (ISR 98-06R)

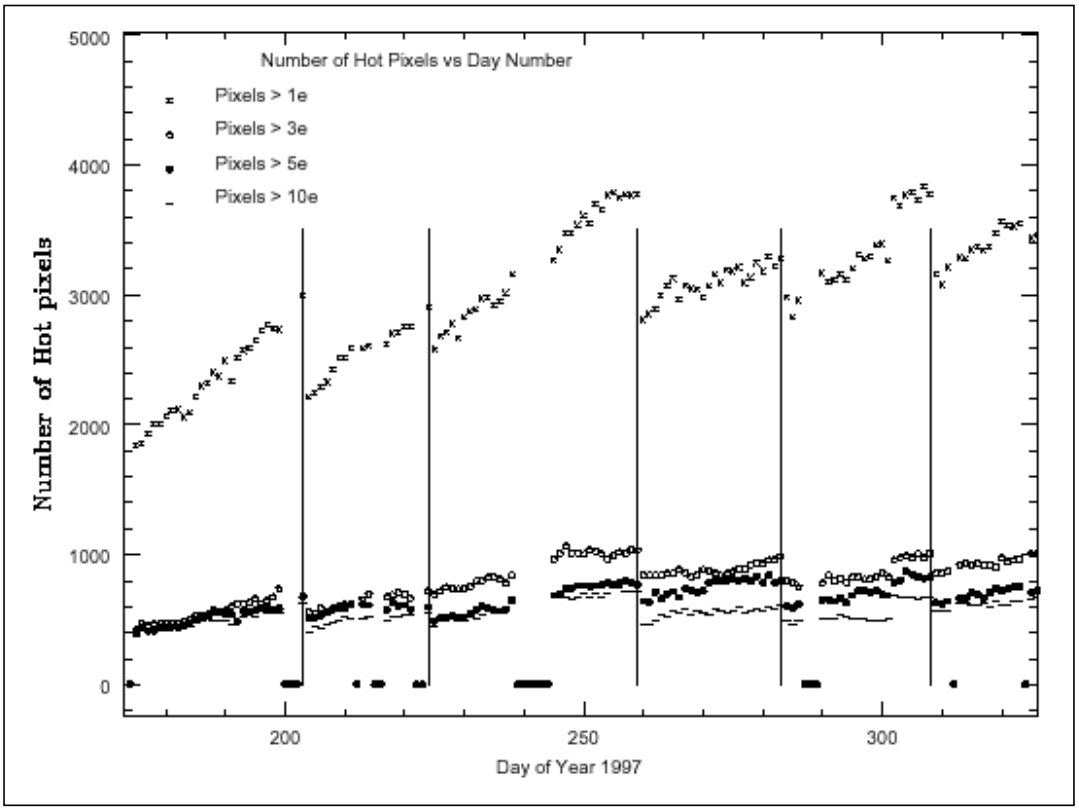

Proposal ID 8056: External Check of Sparse Field CTE

Execution	Executed once on Jun. 4, 1999.
Summary of Goals	Measure the charge transfer efficiency (CTE) using the sparse field test, along both the serial and parallel axes.
Summary of Analysis	The analysis includes results from proposal 7666. The analysis is discussed in Goudfrooij 2000 (see Fig. 7), Gilliland *et al.* 1999, and Kriss 1999. Results were presented at the Workshop on Hubble Space Telescope: CCD Detector CTE Jan. 31 - Feb. 1, 2000, held at STScI (*http://www.stsci.edu/instruments/acs/ctewg/cte_workshop.html*). Also, refer to the IHB, ch. 7.
Accuracy Achieved	CTE performance loss of 1% for signal levels of 100-200 electrons at the center of the chip.
Continuation Plans	Continued in proposal 8415.

Figure 7: Pre-launch ground tests showed excellent CTE performance with losses of about 1% for signal levels of 100-200 electrons at the center of the chip. One year after launch about 6% CTE loss was measured at the center of the chip at count levels of 100 electrons. After 2.5 years on orbit the CTE loss at the chip-center showed about 10-20% increase at 100 electrons signal levels. Low sky levels (about 10-20 electrons) appear to decrease the loss by a factor of two. (Kriss 1999) **Left:** Comparison of external CTE tests for the CCD (proposal 8056 measurements represented by squares). **Right:** Parallel charge transfer inefficiency (CTI) is given by the slope of Amp D/Amp B intensity ratio versus the position on AXIS2, as shown by these two plots for different signal levels. (Goudfrooij 2000)

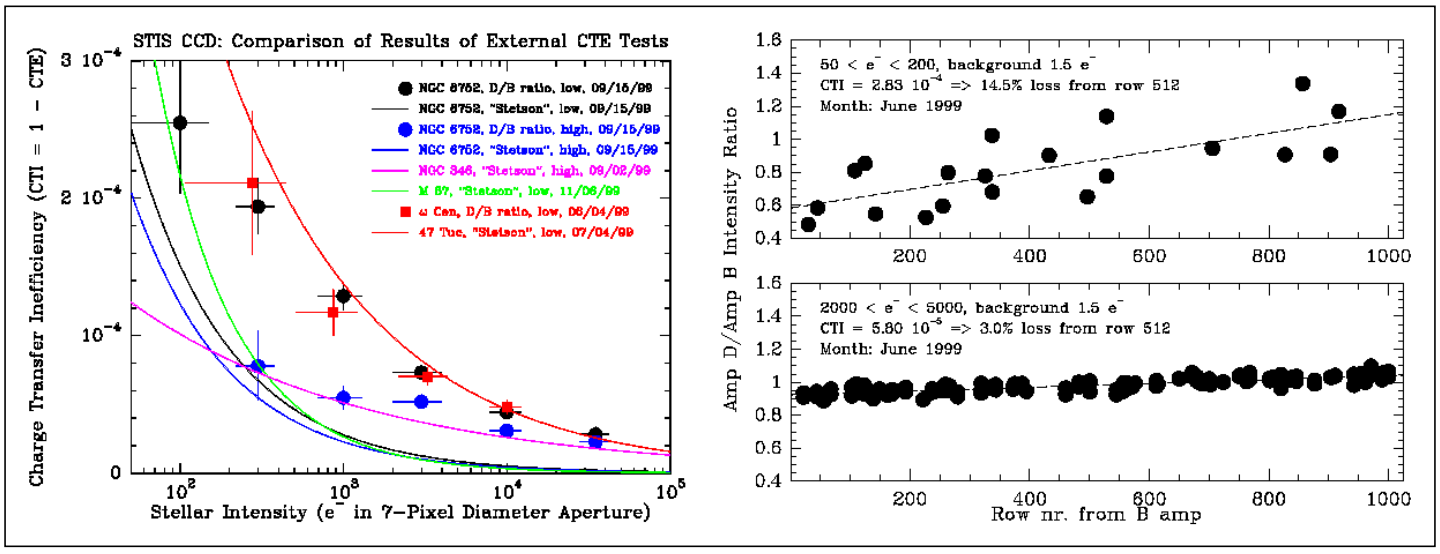

3. MAMA Monitoring and Detector Calibration

Proposal IDs 7604, 7950: MAMA Dark Monitor

Execution	Proposal 7604: 5 times per week and 7950: 2 times per week.
Summary of Goals	Characterize the dark current versus temperature for the MAMAs.
Summary of Analysis	Refer to Fig. 8 and IHB, ch. 7. MAMA dark current analysis is included in the ISR 99-02. The FUV-MAMA dark current is best analyzed in IDT Post-Launch Quick-Look Analysis Reports 057 and 037.
Accuracy Achieved	FUV dark count rate: typically 7 counts/sec across the detector, but varies with the detector temperature, particularly in one region of the detector, as shown in Fig. 8 (right). Dark current in the low area stable to ~10% over time. NUV dark count rate: 800-2000 counts/sec, varying both with the temperature and past thermal history of detector, with time, and varies slowly across the face of the detector, by about 1.25 times from center to lower left corner.
Continuation Plans	Continued in Cycle 8 as part of proposal 8426.

Figure 8: Left: NUV-MAMA dark current versus temperature measured from dark images during Oct. 1997 to Apr. 1998. The NUV-MAMA dark current comes from phosphorescence of impurities in the MgF_2 detector faceplate. **Right:** The FUV MAMA dark current as a function of time in high and low regions. The source of the FUV-MAMA dark current is intrinsic to the micro-channel plate. The inset shows the variation across the detector, particularly in the upper left quadrant, pixels [200:400,600:800], which has the higher dark current. (IHB, ch. 7, Fig. 7.9, 7.10, 7.11)

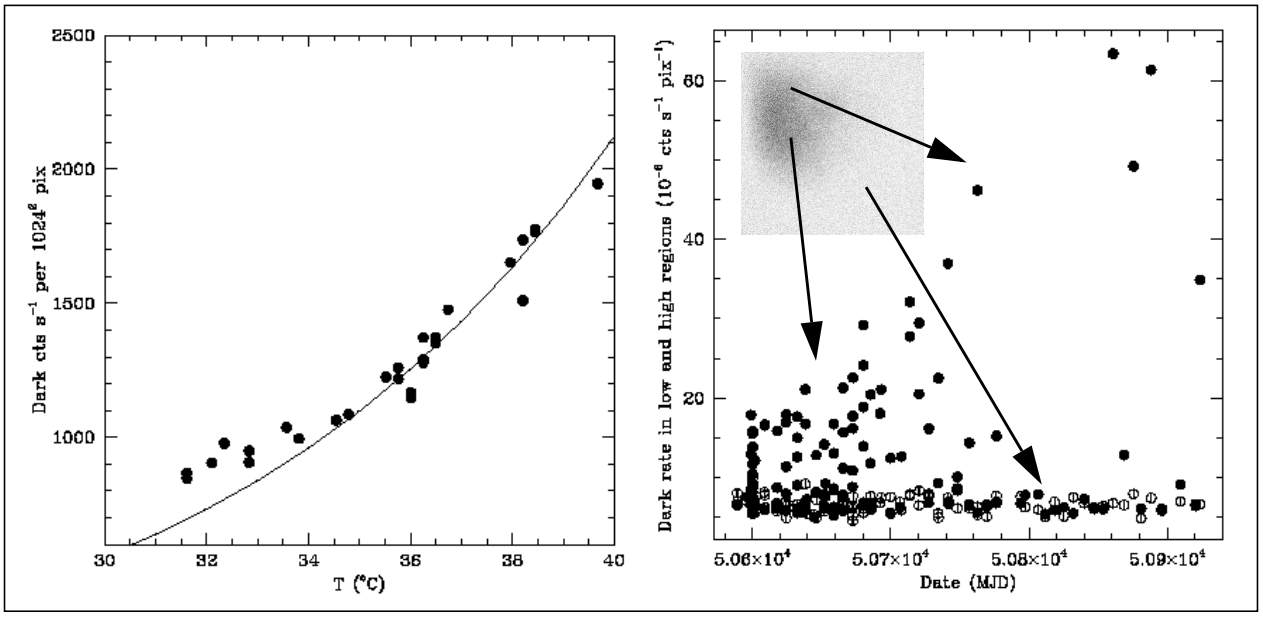

Proposal IDs 7644, 7728: NUV-, FUV-MAMA Monitoring Flats

Execution	Executed about 8 times per Cycle for each camera.
Summary of Goals	Quantify the lamp output and lamp lifetime. Monitor delta flat-fields for the MAMA detectors and compare pre-launch flat-field characteristics with those observed on orbit.
Summary of Analysis	The analysis is given in the ISR 98-15 (see Fig. 9). Also refer to Kaiser *et al.* 1998. Products include reference file updates (pfl).
Accuracy Achieved	1% accuracy per pixel for the proposal 7644 and 2% accuracy per low-resolution pixel for the proposal 7728.
Continuation Plans	Not included in Cycle 8 calibration plans.

Figure 9: Right: spectral response of the Kr and D_2 lamps. **Left:** the decline of Krypton (triangles) and Deuterium (squares) lamp output since Aug. 1997. The output of the flat-field lamps has declined about 15% to 20% in less than 12 hours of on orbit use. Extrapolating the D_2 lamp output with an exponential decay function put the lamp output at 50% after 37 hours of use, at 20% after 87 hours, and at 5% after 165 hours. A linear fit for the the D_2 lamp output predicts zero output after 75 hours of use. The decline in the Kr lamp is harder to predict but is similar to the D_2 curve if an accumulation of contaminants is responsible for the degradation. These estimates are well below the 475 hour (Kr) and 740 hour (D_2) lifetimes expected from pre-launch vacuum testing. (ISR 98-15)

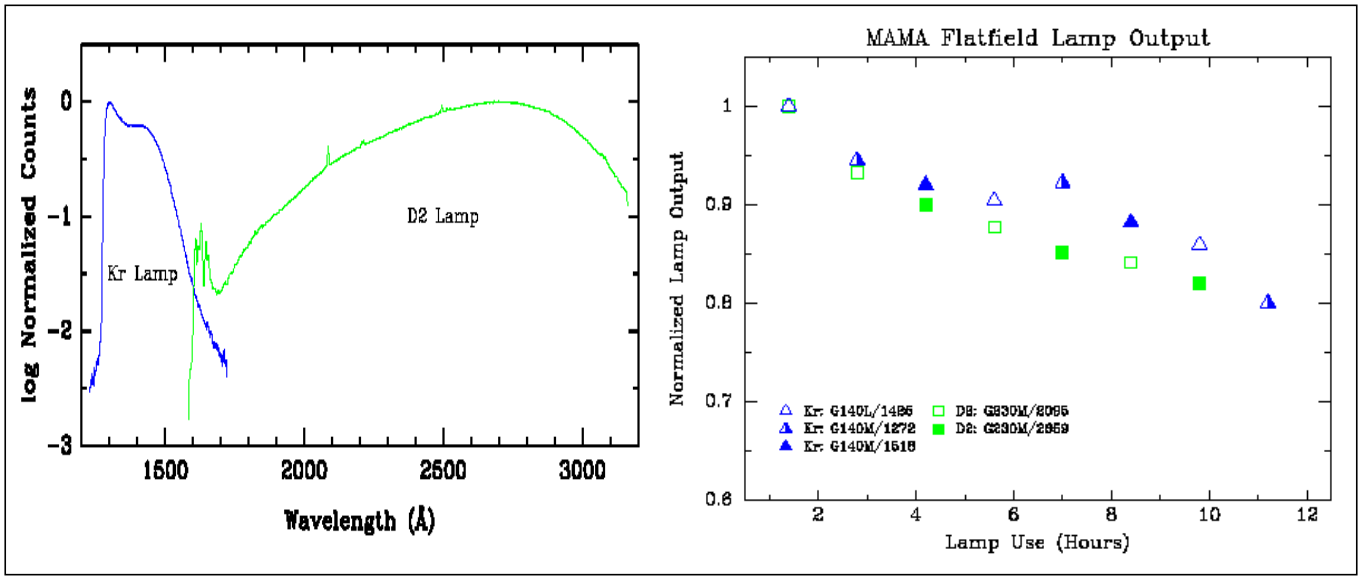

Proposal IDs 7645, 7647: FUV-, NUV-MAMA Flats

Execution	Executed about 11 times between Mar. and Aug. 1998, however, proposals designed to execute 1-2 times per week. HOPRs filed against two visits (one visit in proposal 7645 and another in 7647), which were not approved to be rescheduled.
Summary of Goals	Monitor MAMA pixel-to-pixel flat-field characteristics.
Summary of Analysis	The analysis is given in Ferguson 1998 (see Fig. 10) and Kaiser *et al.* 1998. Products include the reference files: ibn18109o_pfl (also using data from proposal 7644) for the NUV-MAMA and ibn1813ro_pfl for the FUV-MAMA. The pre-launch analysis for the NUV-MAMA flat-fields discussed in the ISR 97-07.
Accuracy Achieved	The MAMA flats have shown some evidence for variation at the ~1-2% per year per resolution element (IHB, ch. 16).
Continuation Plans	Continued in Cycle 8, proposal 8428 for the FUV-MAMA flats and proposal 8429 for the NUV-MAMA flats.

Figure 10: A portion of the preliminary FUV-MAMA high S/N flat. The tightly woven grid pattern is due to sensitivity variations between high-resolution pixels. These variations are due mostly to the way the MAMA detectors centroid the individual charge clouds, that is, counts are being re-distributed between adjacent pixels rather than being lost. These variations largely go away when the data is binned into the standard low resolution mode (1024x1024 pixel format) used by most observers. The hexagonal grid pattern is due to the way the fiber-optic cables are stacked in the MAMA manufacturing process. The wavy pattern is a beat pattern between the pores of the micro-channel plate and the anode array. The diagonal stripe is the shadow of the FUV-MAMA repeller wire, which is masked in the reference files. (Ferguson 1998)

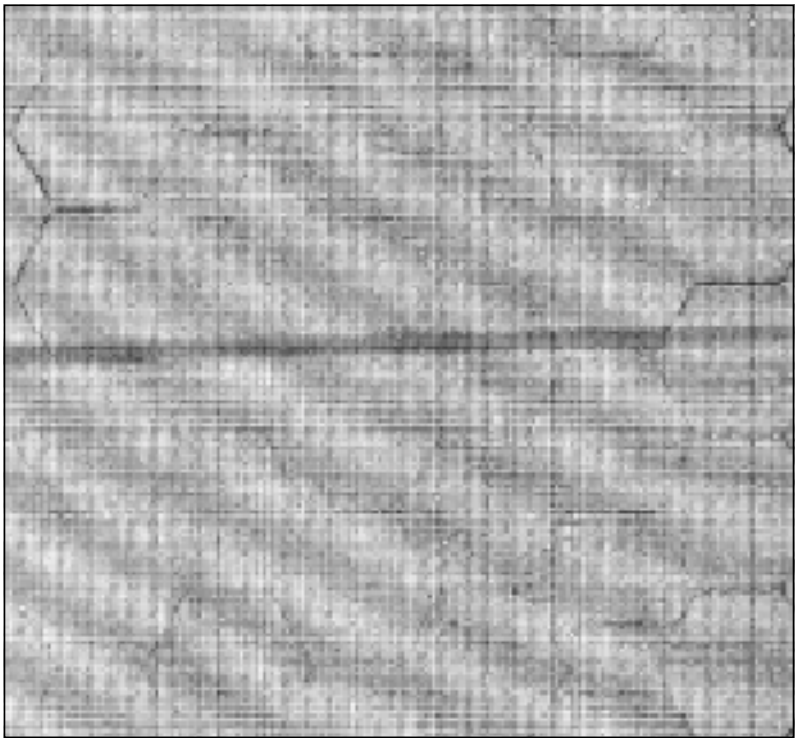

Proposal ID 7670: MAMA Ramp-up Test

Execution	Executed during Nov. 1997. Target was not acquired in the aperture. Two orbits executed, for which HOPRs were filed but the orbits were not repeated.
Summary of Goals	Measure the stability of the count rates on both MAMA detectors immediately after leaving the SAA and turning on the high-voltage.
Summary of Analysis	Analysis was not completed since the target was not acquired in the aperture. However, the background variation was analyzed over 10 second intervals (i.e., geocoronal Lyman-alpha). Results show a steady decrease in the background counts, which is likely due to the increasing distance from the SAA. (STIS Quick-Look Analysis Report 7670) Earlier analysis available in the TIR 97-05.
Accuracy Achieved	Not available.
Continuation Plans	Not included in Cycle 8 calibration plan.

Proposal ID 7937: MAMA Off-Axis Sensitivity (Vignetting)

Execution	Four orbits executed in Feb. 1999.
Summary of Goals	Follow-up previous proposals (SMOV and Cycle 7 calibration) to measure the STIS relative response to a point source in the G430L, G140L, and G140M modes along the slit direction. Observe the stellar targets G191B2B and GD71 at multiple positions along the slit.
Summary of Analysis	Earlier measurements show that there is some vignetting but do not provide an adequate calibration. ISR in progress (N. Walborn).
Accuracy Achieved	Not available.
Continuation Plans	Not included in Cycle 8 calibration plan.

Proposal ID 7965: MAMA Fold Analysis for Cycle 7

Execution	Executed during Nov. 1998 and May 1999.
Summary of Goals	Measure the distribution of the charge cloud sizes incident upon the anode to monitor the health of the micro-channel plates.
Summary of Analysis	No degradation is apparent (see Fig. 11). The analysis is described by Long (1999b). Procedures and requirements available in the TIR 97-09 and ISR 98-02R.
Accuracy Achieved	Degradation is measured as a large (more than 20%) deviation between current and previous measurements.
Continuation Plans	Continued in the Cycle 8 proposal 8427, MAMA Fold Distribution.

Figure 11: The fold analysis measures the health of the MAMA micro-channel plate. When a photon strikes the MAMA detector it frees a single electron, which accelerates through the micro-channel plate and causes an avalanche of other electrons. The resultant cloud of electrons is collected at the coding electrodes and is interpreted as an event. The distribution of this electron cloud on the electrodes is referred to as the fold. Changes in the fold distribution would indicate a change in the condition of the MAMA tube. The plots for the NUV-MAMA (left) and FUV-MAMA (right) consistently show less than 20% change for the fold number distribution, confirming that the MAMA performance as monitored by the fold analysis has not degraded. The Ball Aerospace (Ball) and GSFC measurements are pre-launch. (Long 1999b)

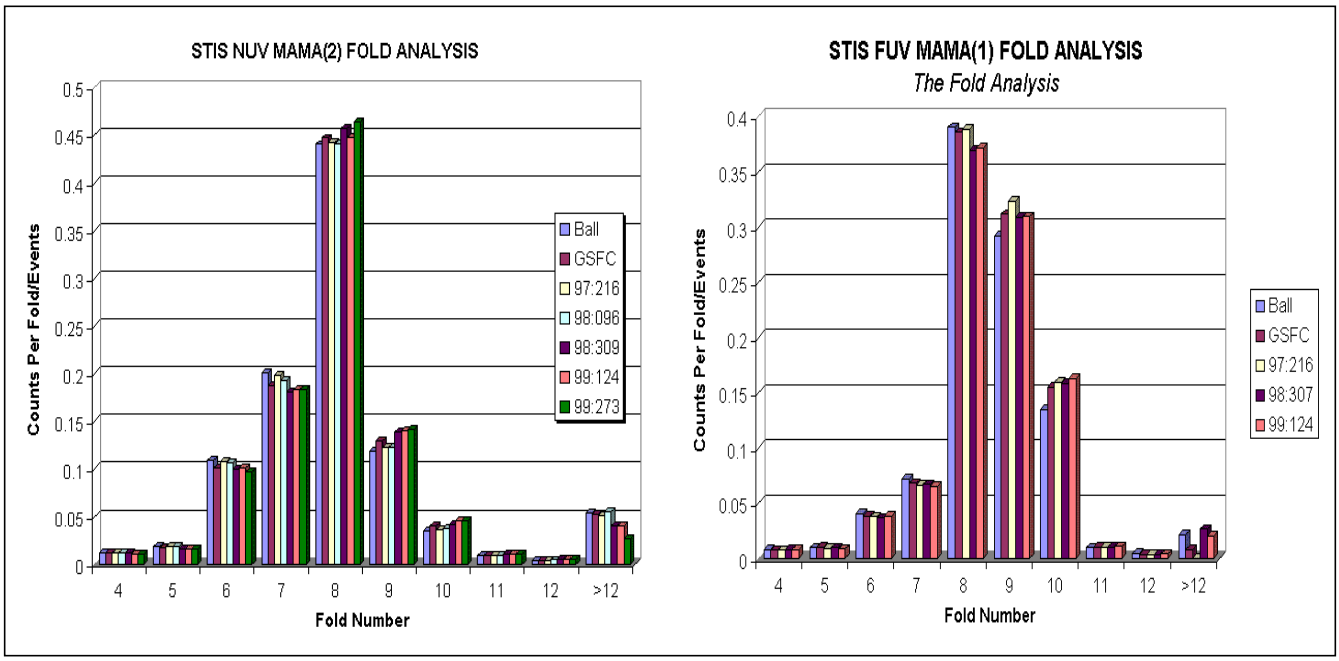

4. Spectroscopic Wavelength and Geometric Distortion

Proposal ID 7648: Missed CCD Dispersion Solutions

Execution	Executed as planned on Sept. 29, 1997.
Summary of Goals	Obtain dispersion solutions for the observing modes G230LB and G230MB.
Summary of Analysis	The analysis is reported in the ISR 98-23 and STIS Quick-Look Analysis Report 7648. The products include reference file updates (j1c1746jo_dsp) for the G230LB and G230MB observing modes. Software requirements for revised dispersion solutions described in the TIR 99-03.
Accuracy Achieved	Calculated and measured dispersions at the nominal central wavelengths agree with the measurements to within ~0.1%.
Continuation Plans	Cycle 8 proposal 8413.

Proposal ID 7649: Missed MAMA Dispersion Solutions

Execution	Executed as planned during Dec. 1997.
Summary of Goals	Obtain dispersion solutions for 9 settings, using the 0.1X0.09 slit, including E230M (1978 Å, 2707 Å), E230H (1763 Å, 2263 Å, 2762 Å, 3012 Å, 2812 Å), E230H (3012 Å with the 0.1x0.03 slit) and E140H (1416 Å) with the Jenkins slit.
Summary of Analysis	The analysis is given in the IDT Post-Launch Quick-Look Analysis Report 062. The products include dispersion solutions and reference file updates (dsp). Software for the revised dispersion solutions described in the TIR 99-03.
Accuracy Achieved	The *rms* values range from 0.16 to 0.27 (STIS Quick-Look Analysis Report 7649).
Continuation Plans	Cycle 8 proposal 8430.

Proposal ID 7650: CCD Dispersion Solution Check

Execution	Once per year on Mar. 1, 1998 and Jan. 31, 1999.
Summary of Goals	Obtain deep engineering wavelength calibration images for all CCD gratings (G750L, G750M, G430L, G430M, G230MB, G230LB) at several wavelength centers.
Summary of Analysis	The analysis reported in the ISR 98-23. Products include reference file updates (j1c1746jo_dsp) and software for revised dispersion solutions described in the TIR 99-03.
Accuracy Achieved	Dispersions at the nominal central wavelengths agree with the measurements to within ~0.1%.
Continuation Plans	Cycle8 proposal 8413.

Proposal ID 7651: MAMA Dispersion Solution Check

Execution	Once per year on Feb. 1998 and Jan. 1999.
Summary of Goals	Obtain dispersion solutions for the E140M, E140H, E230M, E230H, G140M, G140L, G230L, G230M modes.
Summary of Analysis	The MAMA first-order modes were updated using Cycle 7 data, including proposal 7651, except for G140L (the last update from proposal 7095). Analysis showed that the G140L mode did need to be updated. The echelle mode updates are described in the IDT Post-Launch Quick-Look Analysis Report 062. Software for revised dispersion solutions described in the TIR 99-03.
Accuracy Achieved	Not available.
Continuation Plans	Cycle 8 proposal 8430.

Proposal ID 7652: LSF Measure of the CCD-Spectroscopic Modes

Execution	Executed as planned on Mar. 7, 1998 and Feb. 5, 1999.
Summary of Goals	Obtain LSF measurements of an external target using the CCD spectroscopic L and M modes.
Summary of Analysis	Reference file updates not required since the measurements are consistent with those reported in the ISR 98-04 using internal sources. The data also used in the analysis of the calibration proposal 7937 (ISR 99-01). Also refer to the IHB, ch. 13 and ISR 98-04 (SMOV proposal 7077).
Accuracy Achieved	FWHM uncertainty: 2 ± 0.2 pixels (10%). FWHM *rms*: ~2-3%.
Continuation Plans	Not continued during Cycle 8 calibration.

Proposal ID 7653: LSF Measure of the MAMA-Spectroscopic Modes

Execution	The target Hen 1357 (Stingray Nebula) was observed on Nov. 6, 1997 and Apr. 12, 1999. A second target, HD28497, executed on Jan. 9, 1998 and Jan. 30, 1999.
Summary of Goals	Obtain LSF measurements of an external target using the MAMA spectroscopic first order modes.
Summary of Analysis	Reference file updates not required since the measurements are consistent with internal LSF measurements (ISR 98-04). Further analysis is ongoing combined with Cycle 8 proposal 8435. Also refer to the IHB, ch. 13 and ISR 98-04 (SMOV proposal 7078).
Accuracy Achieved	FWHM uncertainty: 2 ± 0.2 pixels (10%). FWHM *rms*: ~2-3%.
Continuation Plans	MAMA echelle LSF measurements continued in Cycle 8, proposal 8435.

Proposal ID 7654: CCD Slitless Spectroscopy

Execution	Executed as planned on Feb. and Jul. 1998.
Summary of Goals	Calibrate the dispersion solution and the sensitivity as a function of the target position using slitless spectroscopy. Apart from a constant shift, the coefficients of the dispersion solution may depend on the position of the target on the detector in slitless mode. Determine the constant shift as well as the change in the dispersion coefficients. In some modes, particularly in the echelle modes, the sensitivity can have a dependence on the position of the object on the detector, which should also be determined.
Summary of Analysis	The analysis is in progress, combined with the Cycle 8 proposal 8434. Description of the slitless mode is discussed in the IHB, ch. 12 (see Fig. 12). A product developed for slitless spectroscopy analysis is the IRAF task *slitless*.
Accuracy Achieved	Not available.
Continuation Plans	Cycle 8 proposal 8434.

Figure 12: Schematic slitless spectrogram of a planetary nebula (IHB, Fig. 12.1).

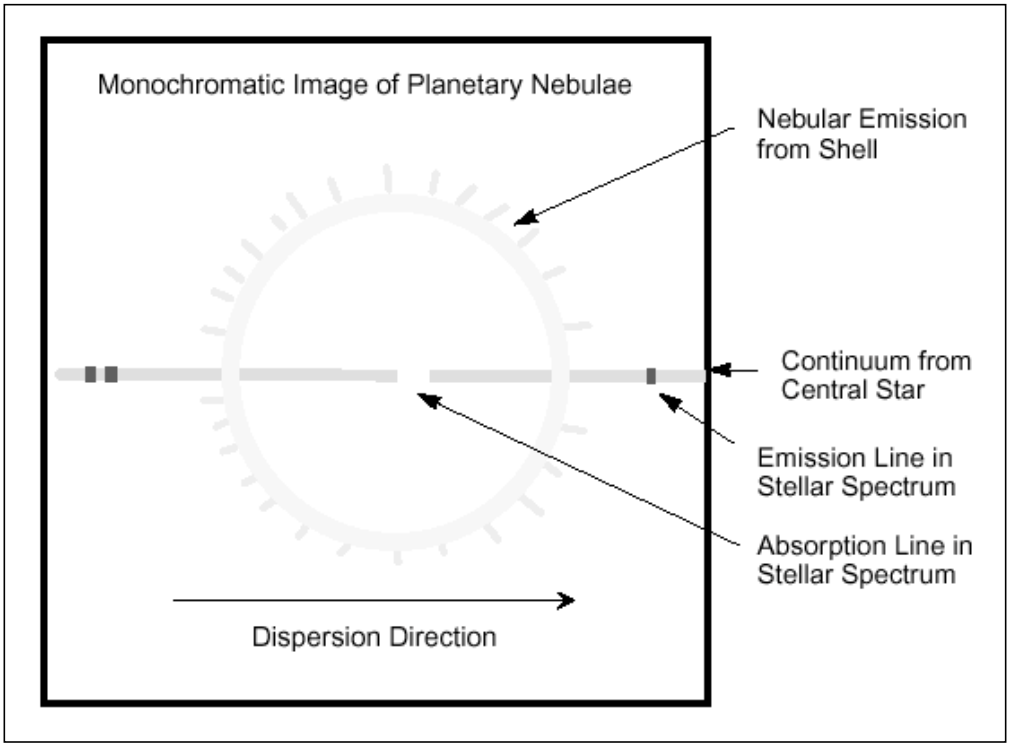

Proposal ID 7665: CCD Geometric Distortion

Execution	Executed on Feb. 13, 1998.
Summary of Goals	Derive the geometric distortion of the CCD first-order spectra for those cases that were missed in ground calibration (G230LB, G230MB modes at 1854 Å).
Summary of Analysis	In the CCD the distortions are less than 1 pixel across the detector (IHB, ch. 14). Spectroscopic spectral traces complete and in the process of being implemented in a reference file (sdc). A TIR in progress (B. Espey & R. Gilliland). Refer to the IHB, Table 14.35, as well as, Malumuth & Bowers 1997.
Accuracy Achieved	The current (IHB, Table 14.35) CCD geometric distortion coefficients were derived using dithered observations of a star field, and tested by rectifying and registering WFPC-2 PC images and STIS images of 47-TUC. The agreement is good to about 0.5 pixels across the chip (and it is not clear whether the remaining 0.5 pixel uncertainty is in the WFPC-2 solution or the STIS solution).
Continuation Plans	Not continued in Cycle 8.

Proposal ID 7667: MAMA Geometric Distortion

Execution	Executed as planned on Sept. 2, 1997.
Summary of Goals	Determine the first-order spectra shape for the MAMAs, which were not included in the ground calibration (G140L, G230L, G140M modes). The extraction of first order spectra requires knowledge of the spectral shape (cross-dispersion offset along the dispersion direction) as a function of where along the cross-dispersion direction the star is initially placed.
Summary of Analysis	For the MAMA the distortions are larger than for CCD, approaching 3 pixels at the corners of the detectors (IHB, ch. 14) Spectroscopic spectral traces complete and in the process of being implemented in reference files (sdc). A TIR is in progress (B. Espey & R. Gilliland). Refer to the IHB, Table 14.35, as well as, Malumuth & Bowers 1997.
Accuracy Achieved	Not available.
Continuation Plans	Not continued in Cycle 8.

Proposal ID 7668: Incidence Angle Correction for Non-Concentric Slits-CCD

Execution	Executed as planned on Oct. 6-7, 1997.
Summary of Goals	Incidence angle corrections for CCD observations using non-concentric slits, which were missed during ground testing calibration.
Summary of Analysis	Reference file updates (iac) are deferred since measured data matches closely with model data. Last reference file (iac) update in May 1997, based on model data (C. Bowers), see Fig. 13.
Accuracy Achieved	Not available.
Continuation Plans	Not included in Cycle 8.

Figure 13: CCD incidence angle correction coefficient values (NCOEFF1 = 1, all other coefficients are 0). The coefficients for the different modes are from the reference file h5s11397o_iac, based on pre-launch and model data (C. Bowers).

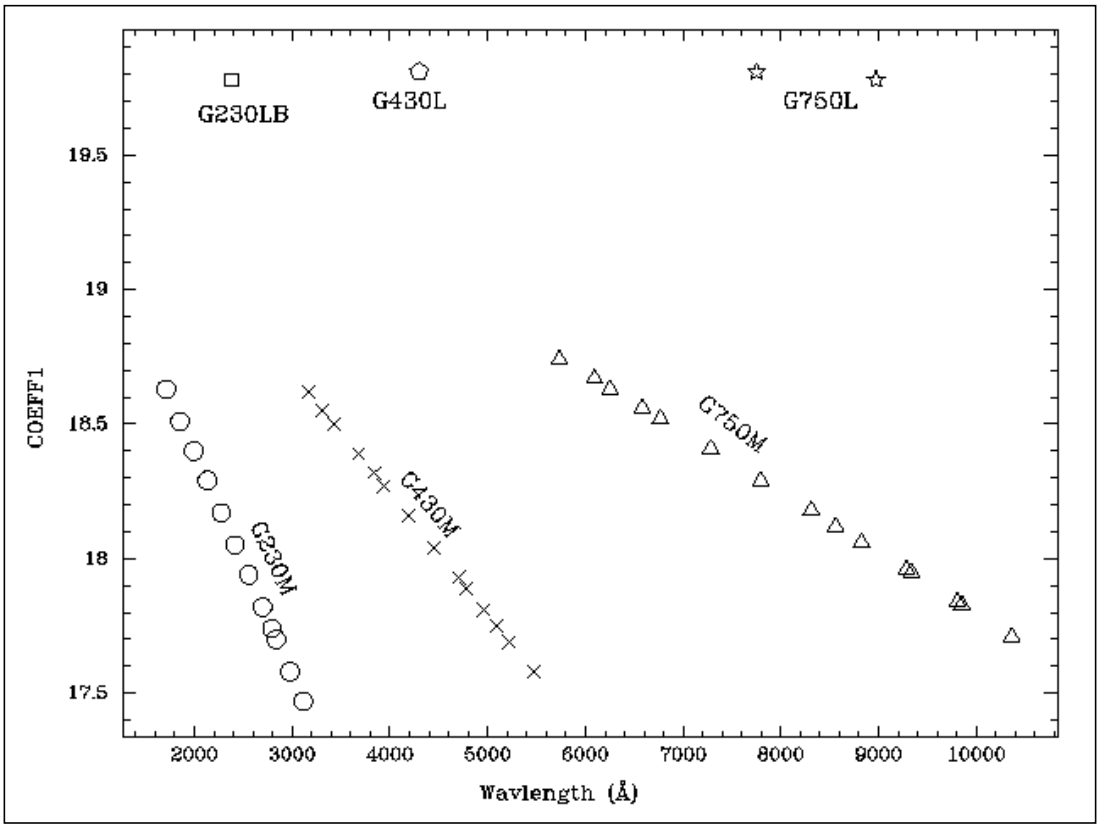

Proposal ID 7669: Missing MAMA Incidence Angle Correction

Execution	Executed during Oct. 1997.
Summary of Goals	Measure the incidence angle corrections for MAMA observations using non-concentric slits with modes missed during ground testing calibration.
Summary of Analysis	The analysis superseded by Cycle 8 proposal 8433. Reference file updates (iac) in progress. Last reference file (iac) update in May 1997, based on model data (C. Bowers), see Table 8.
Accuracy Achieved	Not available.
Continuation Plans	Cycle 8 proposal 8433.

Table 8. MAMA coefficients for all wavelengths and orders, based on prelaunch and model data last updated by C. Bowers (May 1997).

Mode	FUV-MAMA NCOEFF1	COEFF1	Mode	NUV-MAMA NCOEFF1	COEFF1
G140L	1	41	G230L	1	41.6
G140M	1	32.7	G230M	1	31.7
E140M	1	27.8	E230M	1	30.3
E140H	1	21.5	E230H	2	-132.69
X140M	1	34.5	X230M	1	34.5
X140H	1	34.5	X230H	1	34.5
			PRISM	1	34.5

Proposal ID 7936: External to Internal Wavelength Correction

Execution	Executed as planned during Apr. 1997.
Summary of Goals	Characterize the degree of the wavelength offset for an external source from that determined by the internal wavelength calibration system.
Summary of Analysis	The analysis is reported in the ISR 99-01 (refer to Table 9). A different target, Hen 1357 (Stingray nebula), was used for measurements (proposal 7652). Also, the line centers from HDF-S QSO first-order and echelle mode observations were compared with the UCLES instrument at the AAT. Reference file updates were not required. The data from this proposal was used in the analysis of other calibration programs, including proposals 7652 and 7653, LSF measurements for the CCD and MAMAs.
Accuracy Achieved	Line centers determined within 0.1 pixels or 0.27 Å and 0.06 Å for the G430L and G750L modes respectively. The emission lines were less than 8 km/sec FWHM.
Continuation Plans	Not included the Cycle 8 calibration plan.

Table 9. The results for the line centers from the Stingray nebula observations, using G430L (2900 - 5700 Å) and G750M (6295 - 6867 Å) modes (ISR 99-01).

Line ID	λrest (Å)	λobs (Å)	λexp (Å)	λobs - λexp (Å)
Hβ	4862.74	4862.36	4862.95	0.11
[OIII]	4960.29	4960.31	4960.50	-0.21
[OIII]	5008.30	5008.19	5008.51	-0.32
[NII]	6549.93	6550.26	6550.21	0.05
Hα	6564.64	6564.84	6564.92	-0.08
[NII]	6585.24	6585.49	6585.52	-0.03

5. Spectroscopic Photometry

Proposal ID 7656: CCD Spectroscopic and Imaging Sensitivity

Execution	Executed twice per year: Oct. 1997, May and Nov. 1998, Apr. 1999.
Summary of Goals	Measure the sensitivity for all supported CCD imaging and spectroscopic modes.
Summary of Analysis	The analysis is reported in the ISR 99-07 (refer to Table 10) and the IHB, ch. 5 (see Fig. 14). The products include reference file updates (pht). Data also used for the analysis in the ISRs 98-27, 98-20, 98-01, and Bohlin 2000.
Accuracy Achieved	Spectroscopic accuracy: 2 to 5%, depending on mode. Imaging accuracy: 5%. Accuracies reported in the IHB ch. 16.
Continuation Plans	Spectroscopic sensitivity calibration continued in Cycle 8, proposal 8418.

Proposal ID 7657: MAMA Spectroscopic and Imaging Sensitivity

Execution	Nov. 1997, Jan. 1998, Dec. 1998, Jan., Feb., and Mar. 1999.
Summary of Goals	Measure the sensitivity for all supported MAMA imaging and spectroscopic modes.
Summary of Analysis	Analysis reported in ISR 99-07 (refer to Table 10) and the IHB, ch. 5 (see Fig. 15). Products include reference file updates (pht). The data also used for the ISRs 98-27, 98-20, and 98-01.
Accuracy Achieved	Spectroscopic accuracy: 2 to 8%, depending on mode. Imaging accuracy: 5%. Accuracies reported in the IHB ch. 16.
Continuation Plans	Spectroscopic sensitivity Proposal 8424.

Table 10. Average sensitivity for STIS modes from the ISR 99-07. Time correction applied unless stated otherwise. Refer to ISR 99-07 for details and wavelength dependencies.

Mode	Sensitivity (% per year)	1σ Photometric Repeatability (%)	Comments
G140L, M	-0.8% to -2.8% (greatest loss at shortest wavelengths)	0.44	After temperature correction (sensitivity drops 0.25% for each 1 C increase in temperature). Corrections commonly in the 0.5% range.
G230L, M	1.3% (launch to 1998.7) 0% to -1.9% (1998.7 to 1999.8)	0.15	Losses increase toward longer wavelengths.
G230LB, MB	less than 0.4% change	0.38	Time correction not required.
G430L, M	–0.5% to –0.7%	0.38	For wavelengths long ward of 3300 Å.
G750L, M	less than 0.4% change	0.24	Time correction not required.

Figure 14: STIS CCD clear and filtered throughputs (IHB, Fig. 5.2).

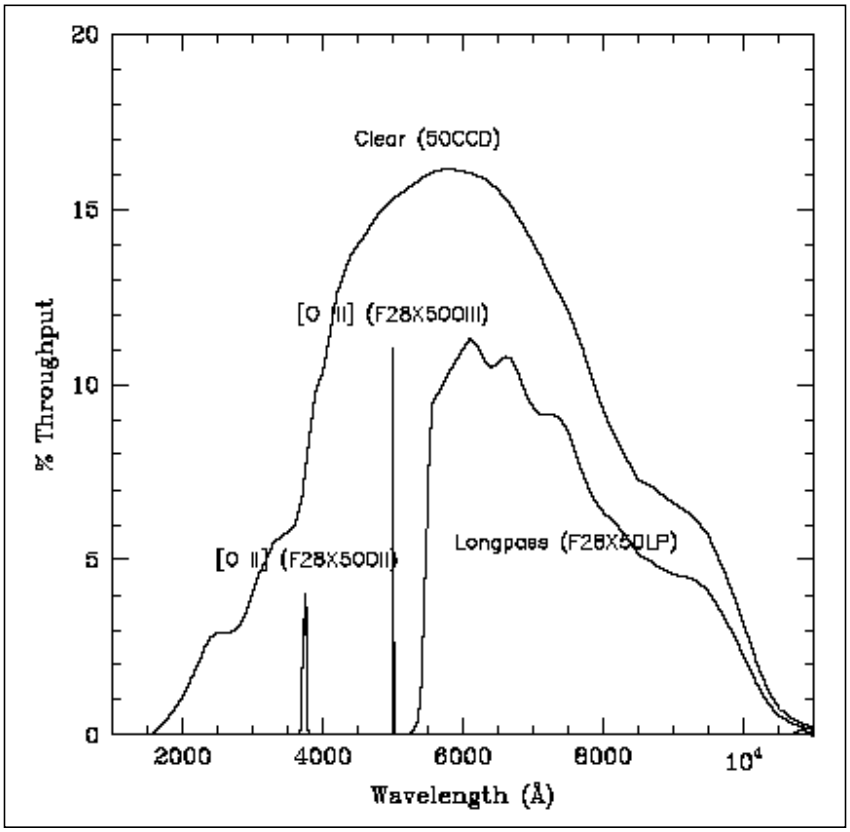

Figure 15: Left: STIS NUV MAMA clear and filtered imaging mode throughputs. **Right:** STIS FUV MAMA clear and filtered imaging mode throughputs. (IHB, Fig. 5.3, 5.4)

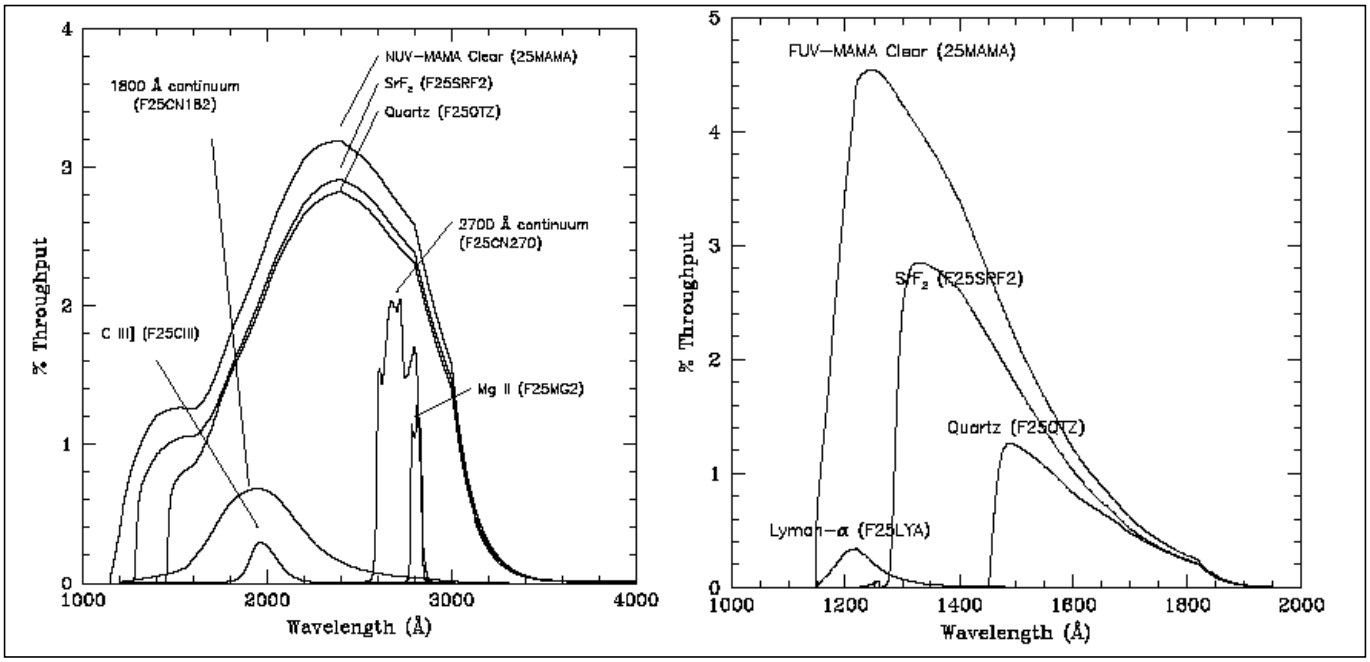

Proposal ID 7672: CCD Contamination/Sensitivity Monitor

Execution	Executed as planned from Aug. 1997 to Jun. 3, 1999: 1 orbit every 2 months for L (low dispersion) modes, 1 orbit every 4 months for M (medium dispersion) modes.
Summary of Goals	Monitor sensitivity of each CCD grating mode to detect any change due to contamination or other causes.
Summary of Analysis	The analysis is reported in the ISRs 99-07, 99-04, and 98-27. Products include reference file updates (pht).
Accuracy Achieved	Average photometric precision over the full wavelength ranges for the 52x2 arcsec. slit given in Table 10.
Continuation Plans	Cycle 8 proposal 8418.

Proposal ID 7673: MAMA Contamination/Sensitivity Monitor

Execution	Executed between Aug. 1997 and Jun. 1999: 1 orbit monthly for L (low dispersion) modes, 1 orbit every 2 months for M (medium dispersion) modes, 2 orbits every 4 months for E (echelle) modes. 1 orbit had guiding problems.
Summary of Goals	Monitor sensitivity of each MAMA grating mode to detect any change due to contamination or other causes.
Summary of Analysis	The analysis is reported in the ISRs 99-07, 98-20, 98-09, and 98-01. Also refer to the IDT Post-Launch Quick-Look Analysis Report 049. Products include reference file updates (pht).
Accuracy Achieved	Average photometric precision over the full wavelength ranges for the 52x2 arcsec. slit given in Table 10 and 0.2x0.2 arcsec. slit for the echelle modes given in Table 11.
Continuation Plans	Cycle 8 proposal 8424.

Table 11. The mean ratio and *rms* scatter, σ_m, of the STIS flux to the standard flux is computed in wavelength bins corresponding to the standard star resolution. Since the mean ratios lie in the range 0.995 to 1.00, any systematic bias from the absorption lines is less than 1% on average. For most of the echelle sensitivities, the uncertainty is NOT limited by the analysis technique but is dominated by the accuracy of the standard star flux and by the photometric repeatability of the observations in the small echelle slits. (ISR 98-18)

Mode	Central Wavelength (Å)	Target	Mean Ratio	σ_m
E140H	1234	BD+75D325	0.995	3.3
E140H	1416	BD+28D4211	0.999	1.3
E140H	1416	BD+28D4211	0.997	1.3
E140H	1598	BD+75D325	0.998	2.9
E140M	1425	BD+28D4211	0.998	1.6
E140M	1425	BD+28D4211	0.998	1.7
E140M	1425	G191B2B	0.996	1.1
E140M	1425	G191B2B	0.996	1.1
E140M	1425	BD+28D4211	0.998	1.7
E230H	1763	BD+75D325	0.995	2.5
E230H	2013	BD+75D325	0.999	0.9
E230H	2263	BD+75D325	0.998	2.2
E230H	2263	BD+28D4211	0.999	0.9
E230H	2263	BD+28D4211	0.999	0.8
E230H	2513	BD+75D325	0.998	1.5
E230H	2762	BD+75D325	0.998	1.2
E230H	3012	BD+75D325	1.000	0.7
E230M	1978	BD+28D4211	0.999	0.8
E230M	1978	BD+28D4211	0.999	1.1
E230M	1978	BD+28D4211	0.999	1.0
E230M	2707	BD+28D4211	0.999	0.7
E230M	2707	BD+28D4211	0.999	0.7
E230M	2707	BD+28D4211	1.000	0.7

Proposal ID 7723: Grating Scatter

Execution	Executed once on Dec. 5-6, 1997.
Summary of Goals	Measure of the grating scattering, if any, using red stars (P330E) at blue wavelengths for the first-order observing modes, G140L, G230L, G230M, G230LB, and G230MB.
Summary of Analysis	Preliminary analysis presented at the AAS in Rochester, June 2000 (Dashevsky & Caldwell 2000) and summarized in the STIS Quick-Look Analysis Report 7723 (see Fig. 16). An ISR is in progress (I. Dashevsky). Scattering model predictions are not available and required for complete analysis.
Accuracy Achieved	Not available.
Continuation Plans	Not included in Cycle 8 calibration plan.

Figure 16: Comparison of overlapping first-order modes using the data from a single star (proposal 7723). The scatter of red photons is shown as increasing the flux in the blue region of the spectrum. Below, the red wavelength region from the G140L mode is compared with the blue wavelength region from the G230L mode data. Notice how the spectrum using the G230L mode deviates from the spectrum of the G140L mode towards bluer wavelengths. Similarly, the CCD G230LB mode is compared with the MAMA G230L mode. The scatter is more prominent in the G230LB mode than the G230L mode since the CCD is more sensitive to red photons. The G230M and G230MB do not appear to be noticeably affected by grating scatter at the long wavelengths shown. (Dashevsky & Caldwell 2000)

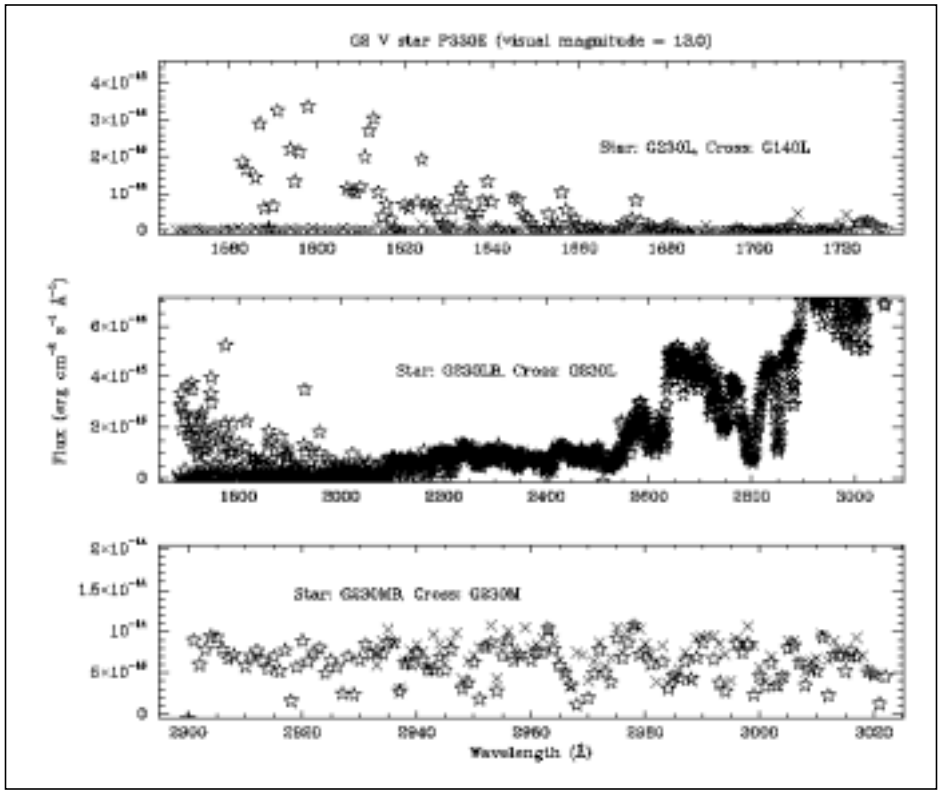

Proposal ID 7805: Contamination: Tie SMOV Stars to Cycle 7 Star

Execution	The star G191B2B was observed on Oct. and Nov. 1997. A second star GD153 was observed on Nov. 1997.
Summary of Goals	Confirm that the change in sensitivity is less than ~1% per year at all CCD wavelengths and compare the stars G191B2B and GD153.
Summary of Analysis	The analysis is reported in Bohlin 2000 (see Fig. 17). Also refer to the ISRs 98-27 and 98-20.
Accuracy Achieved	Residuals with respect to model (LTE) continua are less than ~1% from 2000 to 9000 Å. Total uncertainties in the absolute calibration decreases from 4% at 1300 Å to 2% at 5000-10,000 Å and includes estimates for all systematic effects. The STIS sensitivity in the broad hydrogen lines is uncertain with respect to the adjacent continuum by 2%-3% in the wings and by up to 5% in the line cores.
Continuation Plans	Not included in future Cycles.

Figure 17: Residuals of the STIS calibrated fluxes using three models described in Bohlin 2000. From top to bottom the stars used are G191B2B, HZ43, GD153, and GD71.

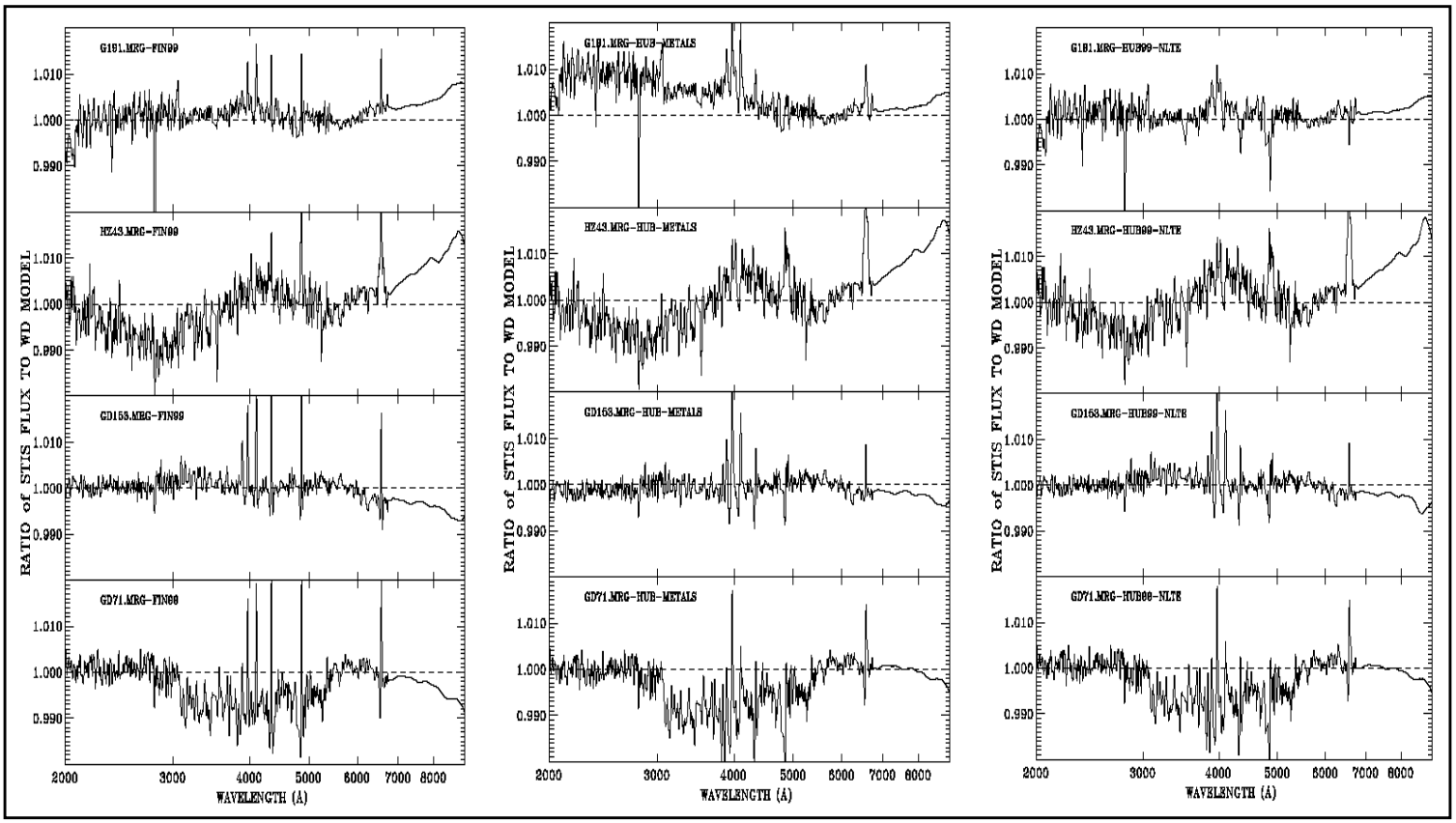

Proposal ID 7674, 8066: IR Standards

Execution	Executed as planned on Sept. and Dec. 1997, Jan., Feb., and Mar. 1998.
Summary of Goals	Establish a set of absolute flux standards on the WD scale that extend the existing wavelength coverage to 10,300 Å with the STIS G750L grating setting.
Summary of Analysis	The analysis is reported in Bohlin 2000. Also, refer to Fig. 17.
Accuracy Achieved	Residuals with respect to model (LTE) continua are less than ~1% from 2000 to 9000 Å. Total uncertainties in the absolute calibration decreases from 4% at 1300 Å to 2% at 5000-10,000 Å and includes estimates for all systematic effects. The STIS sensitivity in the broad hydrogen lines is uncertain with respect to the adjacent continuum by 2%-3% in the wings and by up to 5% in the line cores.
Continuation Plans	Not included in the Cycle 8 calibration plan.

Proposal ID 7809: Prism Sensitivity and Faint Calibration Standard Extensions

Execution	Executed once on May 21, 1998.
Summary of Goals	Measure sensitivity of the prism mode at a central wavelength of 1200 Å with the F25SRF2 filter and the 52x2 apertures, using the faint white dwarf star HS2027+0651.
Summary of Analysis	The analysis is deferred to Cycle 9. The data available in the archive includes: standard target acquisition with the long-pass filter; 6x6 confirmation image; spectra with the G140L, G230L, G230LB, G430L, G750L modes using the 52x2 aperture and another G750L using the 0.3x0.3 aperture for a contemporaneous flat; spectra with the prism using the 52x2 aperture and F25SRF2 filter. The data is suitable for analysis, however, reference files for spectral extraction will need to be updated to include the prism mode before proceeding with measurements. Also refer to the IHB, ch. 14.
Accuracy Achieved	Not available.
Continuation Plans	Cycle 9 calibration will improve wavelength coverage.

Proposal ID 7810: Sensitivity Calibration: Secondary Wavelengths

Execution	Executed once per year on May 21, 1998.
Summary of Goals	Measure the sensitivity at the secondary wavelengths 6581 Å, 8561 Å, for G430M at 4781 Å, for E140H at 1271 Å, and for E230H at 2812 Å.
Summary of Analysis	The analysis is deferred to Cycle 9 due to lack of interest from GO community.
Accuracy Achieved	Not available.
Continuation Plans	Not included in the Cycle 8 calibration plan.

Proposal ID 7917, 8016: Effect of MAMA Charge Offsetting on Sensitivity and Dispersion Accuracy

Execution	Scheduled observations for proposal 7917 failed twice (2 external orbits) and were repeated in proposal 8061 (4 orbits), during July and Aug. 1998.
Summary of Goals	Characterize the effect of offsetting or “dithering” spectra, which may be required to further extend the life of the MAMAs.
Summary of Analysis	The analysis is ongoing with Cycle 8 calibration programs. Also, the data has been used in ISRs 98-27, 98-20, and 98-18, Bohlin 2000 (i.e., sensitivity and other calibration).
Accuracy Achieved	Not available.
Continuation Plans	Not included in future calibration plans.

Proposal ID 7931: MAMA Echelle Scattered Light

Execution	The E140M mode executed in July 9, 1998, G140M, G230M modes executed in Aug. 25, 1998, and H-modes were withdrawn.
Summary of Goals	Quantify the scattering in the echelle observing modes. Another goal not mentioned in the proposal is to correct the scatter.
Summary of Analysis	Refer to Table 12 for results from preliminary analysis. For more analysis refer to Landsman & Bowers 1997. The STIS IDT algorithm for echelle scatter correction (Quicklook Analysis Report 059) has been implemented as an option, called *sc2d*, in the IRAF STIS package X1D task for spectral extraction.
Accuracy Achieved	Before correction the cores of interstellar lines are about -5% of continuum intensity (normalized to unity) for the bluest wavelengths of the E140H and about -1% for the bluest wavelengths of the E230H mode. After correction, using the *sc2d* option, the cores are < 1% of the continuum level. Refer to Table 12 for more details.
Continuation Plans	Complete characterization and documentation of the echelle scattered light and its correction is in progress (J. Valenti).

Table 12. Preliminary results using the standard 1-dimensional and new 2-dimensional corrections for scattered light in the echelle modes. Columns 2 and 3 show the mean flux in the core of a saturated interstellar line, expressed as a fraction (in percent) of the neighboring continuum flux; the uncertainty in these measurements is given in Column 4, which is similar for both types of corrections. The flux change refers to the change in the continuum flux for spectra analyzed with the new 2-dimensional scattered light algorithm, relative to the continuum in spectra reduced with the 1-dimensional algorithm; the corresponding uncertainty values are in the last column.

Optical Element	Wavelength (Å)	1-D Corrected Core Measurement (%)	2-D Corrected Core Measurement (%)	Sigma (%)	Flux Change (%)	Sigma (%)
E140H	1200	-9.0	-1.0	0.4	+4.9	1.1
E140H	1670	-1.5	+0.9	0.1	+1.2	0.6
E140M	1216	-7.4	-0.7	0.5	-0.1	1.1
E230H	1670	-3.3	-0.5	0.2	+1.3	0.7
E230H	2796	-0.6	-0.01	0.05	+1.3	0.7
E230M	1670	+0.2	+0.9	1.9	+1.4	3.1

Proposal ID 7932: Spectral Purity and Slit Throughput, 1st Order

Execution	The targets HD101998 and GD71 executed as planned in Apr. 1998 and GRW+70D5824 executed in May 1998.
Summary of Goals	Calibrate line profiles as a function of slit width and spectral extraction height.
Summary of Analysis	The analysis is given in the ISRs 98-27 and 98-20. Refer to Fig. 18 and the IHB, ch. 13. Also, refer to ISR 97-13.
Accuracy Achieved	CCD throughputs are accurate to within 10%.
Continuation Plans	Not continued in Cycle 8.

Figure 18: Relative throughputs of different STIS spectroscopic modes, where the throughput is defined as the end-to-end effective area divided by the geometric area of a filled, unobstructed, 2.4 meter aperture. (IHB, Fig. 4.3)

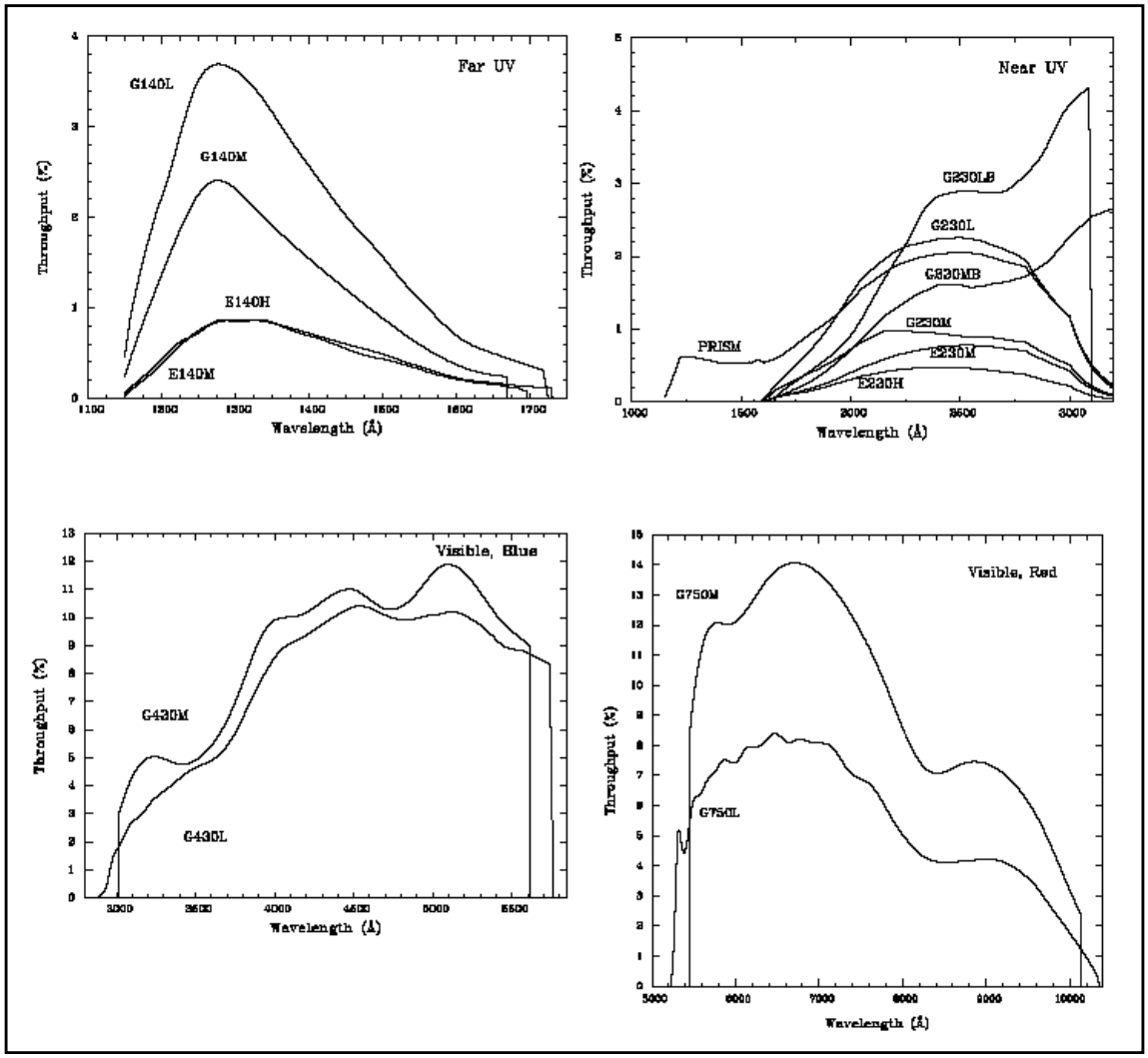

Proposal ID 7943: Transmission of Filtered Echelle Slits

Execution	Executed as planned on Apr. 10, 1998.
Summary of Goals	Transmission measurements of the echelle filtered slits between 1200 Å and 3000 Å using a well-established spectrophotometric standard star (BD+75D325).
Summary of Analysis	The analysis is reported in the ISR 98-25, see Fig. 19 and refer to Table 13. Also refer to the IHB, ch. 13.
Accuracy Achieved	Not available.
Continuation Plans	Not included in Cycle 8 calibration plan.

Figure 19: Transmission of the 0.2x0.05ND (solid) and 0.3x0.05x0.05ND (dashed) filters as a function of wavelength. The depression around 2000 Å might be due to interference in the filters.The filled circles are pre-launch measurements. (ISR 98-25)

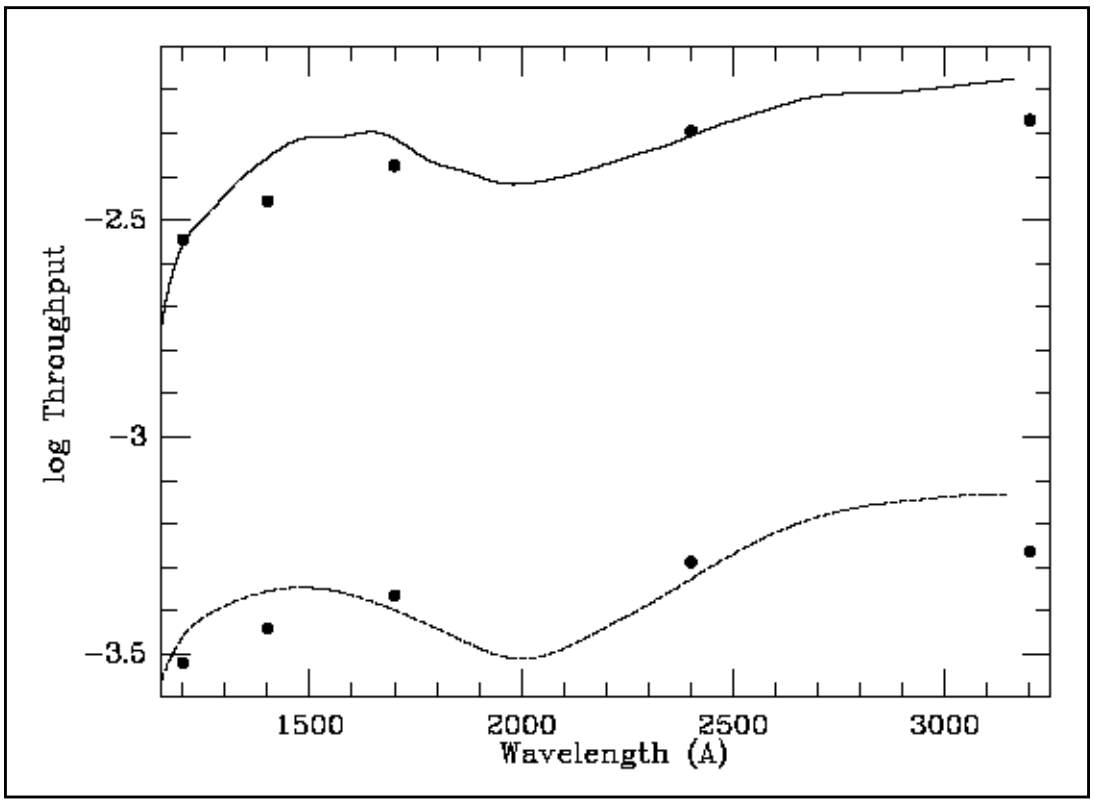

Table 13. Results from ISR 98-25.

Filtered Aperture Name	ND Factors	Logarithmic Attenuation Factors
0.2x0.05ND	100	2.3
0.3x0.05ND	1000	3.3

Proposal ID 8067: E140H Sensitivity Using G191B2B

Execution	Executed once on Dec. 17, 1998.
Summary of Goals	Improve sensitivity measurements for the E140H mode, using G191B2B. Sensitivity has been measured using the star BD+75D325, however, the heavy line-blanketing below 1900 Å confuses the analysis and causes errors of 10-20% in the relative flux within one order (ISR 98-18), see Fig. 20.
Summary of Analysis	The analysis is in progress in conjunction with proposal 7931, Scattered Light in the Echelle Modes. The data also has been used for the ISR 98-18, absolute flux calibration for echelle modes.
Accuracy Achieved	Preliminary results are given in Table 12. After the 2-dimensional correction for the E140H mode the core flux of interstellar lines may be measured to within 1% of the continuum level.
Continuation Plans	Not continued in future Cycles.

Figure 20: The spectrum of the standard star BD+75D325 (top) shows many absorption lines at wavelengths below 1900 Å compared to the spectrum of the standard star G191B2B (bottom).

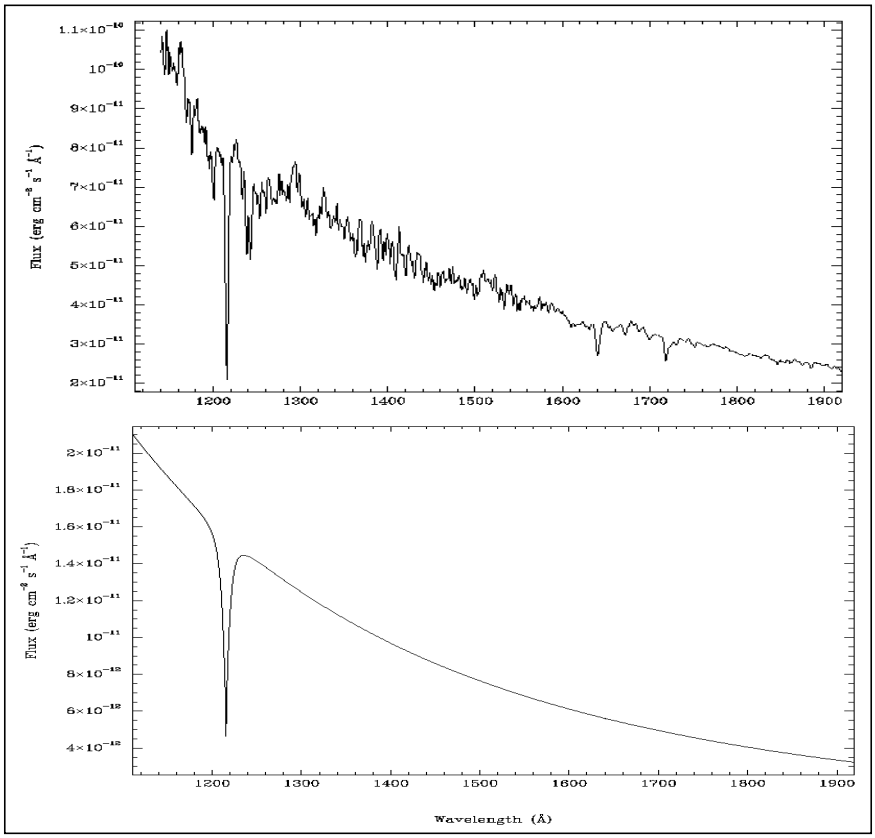

6. Imaging Photometry and Geometry

Proposal ID 7639: CCD Contamination/Sensitivity Over Full Field

Execution	5 executions about 6 months apart, starting Dec. 1997.
Summary of Goals	Measurements of a photometric standard star field in Omega Cen in the 50CCD mode to monitor sensitivity over the whole field of view.
Summary of Analysis	The analysis deferred and combined with Cycle 8 calibration.
Accuracy Achieved	Not available.
Continuation Plans	Continued with 2 executions in Cycle 8 (proposal 8416) at about the same orient as data from 7639.

Proposal ID 7641: CCD External Flats, Stellar

Execution	Executed on Sept. 2, 1997.
Summary of Goals	Measure accuracy of the CCD flat-fielding around dust features on the filters. Observation of the center of 47-Tuc stepped across the detector in very fine steps (0.02 arcsec. in AXIS1 and AXIS2). Attempt to put a relatively bright star at the center of one of the dust motes and step it across.
Summary of Analysis	The target was centered 0.39 arcsec. from where it was supposed to be, however, the data was sufficient for analysis. The photometric stability looked good. The mean magnitudes for 426 stars (ranged in magnitude from AB=14.5 to AB~19) were measured using aperture photometry with a 3 pixel radius in each of 12 frames taken with the 50CCD aperture. The standard deviation of the residuals about these means ranged from 0.007 to 0.012 magnitudes from frame to frame. The mean difference between frames ranged from -0.017 to 0.011 magnitudes. However, since the target was not properly acquired it will be harder to monitor photometry around dust features. (STIS Quick-Look Analysis Report 7641) Also, refer to Ferguson *et al.* 1997. Flat-fielding technical requirements described in the TIR 96-08.
Accuracy Achieved	Using the pipeline flats, relative photometry looks good to better than 0.02 mag., even with fairly crude aperture photometry.
Continuation Plans	Not continued in Cycle 8.

Proposal ID 7642: CCD Red Light PSF Halo

Execution	Executed as planned during Sept. and Oct. 1997.
Summary of Goals	Measurements of the PSF of a red star with the CCD at red wavelengths, to characterize the internal scattering of long-wavelength light within the CCD itself. A red star was observed through the F28X50OIII-CCD filter, taking advantage of the red-leak at greater than 1 micron to get an estimate of the red halo at the longest wavelengths. Also, a star was observed through F28X50LP to characterize the halo at wavelengths more appropriate to observers. Finally, spectra were taken using G750L to characterize the wavelength dependence of the halo.
Summary of Analysis	Ten images were taken in each of three dither positions. The images are unsaturated, and have reasonably high S/N. The F28X50LP images reach 80% of the total flux in an aperture of radius of 3 pixels. In the OIII image (which was being used primarily for its red-leak), 80% of the energy is encircled in a 4 pixel aperture. The PSF itself is flattened with a strong spike in the row direction. The S/N is about 10-40 per lambda pixel in the G750L spectra. The spectra were taken through 52" by 0.1", 0.2", and 0.5" slits. The spectra will have to be fringe corrected before we can assess the effect of the red detector halo on the spectral lines. The contemporaneous flats look fine for this. (STIS Quick-Look Analysis Report 7642) Further analysis is in progress (C. Proffitt).
Accuracy Achieved	Will be available in Cycle 8.
Continuation Plans	Not included in the Cycle 8 calibration plan.

Proposal ID 7661: MAMA Filter Red Leak

Execution	Executed as planned on Apr. 8, 1998.
Summary of Goals	Characterize the red leak, in slitless mode and with the MAMA filters F25CNIII, F25CN182, F25CN270, F25MGII, F25QTZ, F25LYA, and F25SRF2 using the CCD. Also, measure the throughput of the CCD filters F28X50LP, F28X50OII, and F28X50OIII using the gratings G230LB, G430L, and G750L.
Summary of Analysis	The results for the narrow line filters are quite close to previous estimates, but the F28X50LP shows a 25% larger throughput than previous estimates. This discrepancy has not been resolved. (STIS Quick-Look Analysis Report 7661) More analysis is reported in the IDT Quick-look Analysis Reports 023, 016 and 008. Products include reference file updates (apt) for F25SRF2 filter throughput (j781536qo_apt). Also refer to IHB, ch. 14. Low priority was given to the analysis of the red leak data since STIS users have not requested any of the modes in the proposal.
Accuracy Achieved	Measurements agree within 3-5% with previous aperture throughput measurements, except for the F25SRF2 filter that has subsequently been updated, F28X50LP, and F28X50OIII (has overlapping orders at the long wavelength end) filters, which are still being analyzed. Most of the uncertainty is due to systematic effects.
Continuation Plans	F28X50LP filtered mode calibration is continued as part of proposal 8422.

Proposal ID 7666: CCD Linearity and Shutter Stability Test

Execution	4 internal orbits on Nov. 11, 1997 (tungsten lamp flat fields), 2 orbits on Dec. 24 and 29, 1997 (two M67 fields), 1 orbit during the Continuous Viewing Zone on May 5, 1998 (a Cen A and B) at gain = 1, 4.
Summary of Goals	Test for non-linearity in the CCD and its shutter at various combinations of low and high count level, gain, and for imaging and spectral modes.
Summary of Analysis	The analysis is reported in Gilliland *et al.* 1999 (see Table 14), and the ISR 99-05. Also refer to Goudfrooij 2000.
Accuracy Achieved	Shutter stability repeatability quantified to 0.2 milli-seconds. At high count levels, the CCD was shown to have a nearly perfect linear response at gain = 4, even when the saturation of pixels is exceeded. With gain =1, significant deviations from linearity start to occur near and saturation. For low count levels linearity see Table 14.
Continuation Plans	Not continued in Cycle 8.

Table 14. At low count levels there is a position and intensity dependent nonlinearity in the CCD that is believed to be caused by imperfect CTE. **Parallel clocking direction:** The non-linearities between 3.6 and 97.2 second exposures for four stars (in M67, Cycle 7 calibration proposal 7666) placed at different “y” positions (i.e., AXIS2) are given below. Example: The spectrum located at y = 763 is 21% fainter than that for y = 241; the nonlinearity is larger for the star at lower row numbers, despite its being slightly brighter. **Serial clocking direction:** mean difference in linearity between low and high “x” position (i.e., AXIS1) is 2%, which is larger for higher x. (Gilliland *et al.* 1999)

“y” position	Brightness	Nonlinearity (%)	1024 - y
241	1.00	22.6	783
626	0.43	23.4	398
763	0.79	12.3	261
904	0.28	7.2	120

Proposal ID 7720: MAMA Full Field Sensitivity

Execution	Every 6 months: Sept. 1997, Mar. 1998, Sept. 1998, Mar. 1999.
Summary of Goals	To monitor the sensitivity of the FUV-MAMA and NUV-MAMA over the full field.
Summary of Analysis	Analysis deferred, combined with Cycle 8 calibration. Also refer to the IHB, ch. 5.
Accuracy Achieved	Throughputs are good to within 5% for the FUV- and NUV-MAMA.
Continuation Plans	Uninterrupted 6 month time line with two visits in Cycle 8 proposal 8425.

Figure 21: NUV-MAMA image of NGC 6681 (proposal 7720) exposed for 320 seconds, using the F25QTZ filter (IHB, Fig. 5.11).

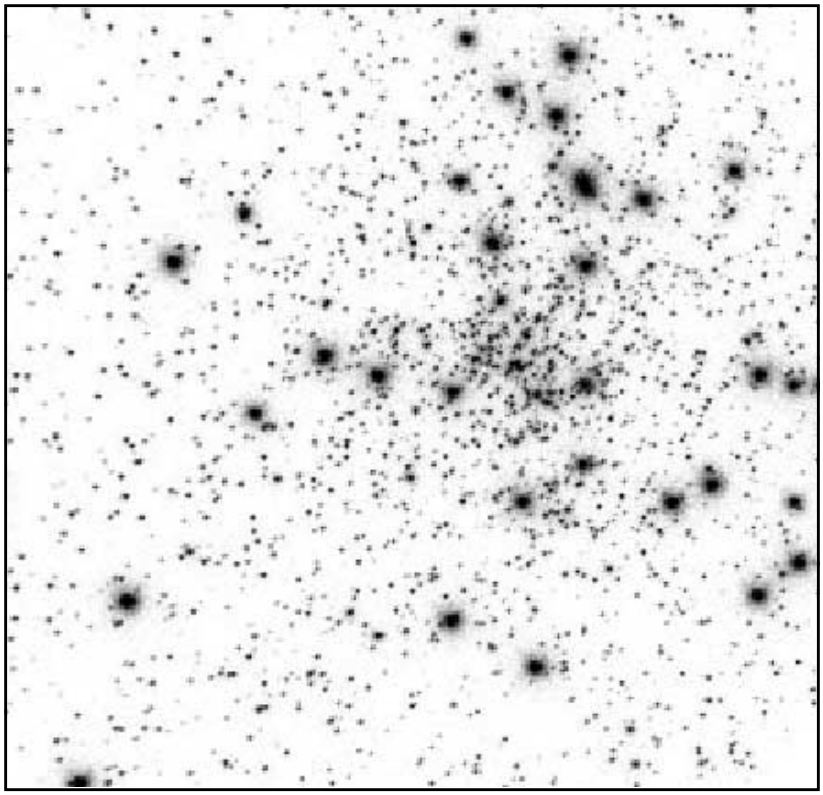

Proposal ID 7774: Deep MAMA PSF Measurement

Execution	Executed as planned on Nov. 25, 1997.
Summary of Goals	Determine the PSF profile as a function of wavelength for the MAMA imaging modes, extending into the wings of the PSF.
Summary of Analysis	Refer to IHB, Figs. 14.92-14.95. The data consists of deep images of isolated point source targets (faint star near brighter star) using the MAMAs in time-tag mode, with the F25LYA, F25CIII, and F25MGII filters, see Fig. 22. Products include reference file updates (apt). An online PSF database is currently being implemented (C. Proffitt). Also refer to the IDT Post-Launch Quick-Look Analysis Report 038, and IHB, ch.'s 7 and 14.
Accuracy Achieved	The fraction of flux enclosed within a 0.05 arcsec. radius aperture varies across the MAMA detectors. For the NUV-MAMA the variation encircled energy varies from 31% to 47% with the F25CN182 filter. Similarly, for the FUV-MAMA the encircled energy varies from 38% to 44% with the F25QTZ filter.
Continuation Plans	Not continued in Cycle 8.

Figure 22: MAMA detector PSFs (IHB, Fig. 7.8).

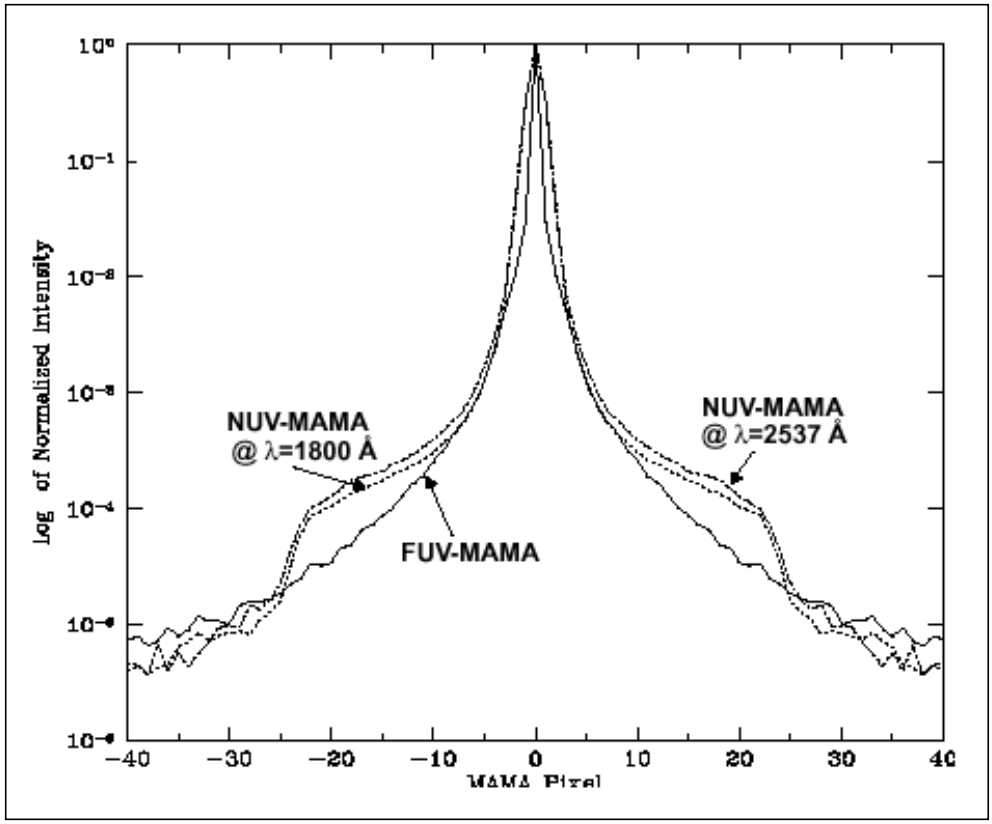

Proposal ID 7788: MAMA Image Location and Geometric Distortion

Execution	Executed on Nov. 6, 1997. Portions of the NUV-MAMA calibration were lost due to an on-board computer problem, which decreased the precision of the plate scale measurements.
Summary of Goals	Measure the image location for each of the MAMA imaging mode, with respect to the CCD frame, as well as the geometric distortion in the NUV-MAMA, using the same field as for the SMOV MAMA PSF test.
Summary of Analysis	Refer to Table 15. Latest analysis in the IHB, ch. 14 (see Table 15). Also refer Malumuth & Bowers 1997 and IDT Post-Launch Quick-Look Analysis Report 051.
Accuracy Achieved	The accuracy of the plate scale measurements is approximately 0.1% for the CCD; 0.04% and 0.08% for the FUV-MAMA, in AXIS1 and AXIS2 respectively; 0.5% and 0.4% for the NUV-MAMA, in AXIS1 and AXIS2 respectively.
Continuation Plans	Not included in Cycle 8 calibration plan.

Table 15. Plate scales at the center of the detector field determined from image mode geometric distortion data. The quoted errors are formal random errors derived from the uncertainties in measuring the positions of the sources. (IHB, pages 410-411)

Detector	AXIS1 Plate Scale (arcseconds)	AXIS2 Plate Scale (arcseconds)	Comment
CCD	0.05071 $\pm$ 0.00007	0.05071 $\pm$ 0.00007	
FUV-MAMA (unfiltered)	0.02447 $\pm$ 0.00001	0.02467 $\pm$ 0.00002	Plate scale is 1.003 times larger for filtered modes (more arcsec. per pixel).
NUV-MAMA (filtered)	0.024547 $\pm$ 0.00013	0.02479 $\pm$ 0.000096	With the F25CN270 filter.

Proposal ID 8069: Throughput of F25ND5 Filter

Execution	Executed as planned on Dec. 12 and 14, 1998. The data is noisey.
Summary of Goals	Measure the absolute sensitivity of the F25ND5 filter.
Summary of Analysis	The analysis is reported in a draft ISR. The apparent measured transmission is approximately $1x10^{-6}$ in both NUV- and FUV-MAMAs, which is a factor of 10 lower than the nominal transmission expected for this filter (Ferguson *et al.* 1999). Products include the IHB update for Cycle 10 the reference file j781536qo_apt (see Fig. 23), as well as, Synphot updates. Also refer to the IHB ch. 5 and ch. 14.
Accuracy Achieved	High NUV-MAMA background makes it very difficult to get an accurate spectral extraction and the FUV-MAMA spectrum is very faint, so the measured transmission has a large uncertainty.
Continuation Plans	Not included in the Cycle 8 calibration plan.

Figure 23: The throughput for the F25ND5 neutral density filter using the data from proposal 8069 (reference file j781536qo_apt).

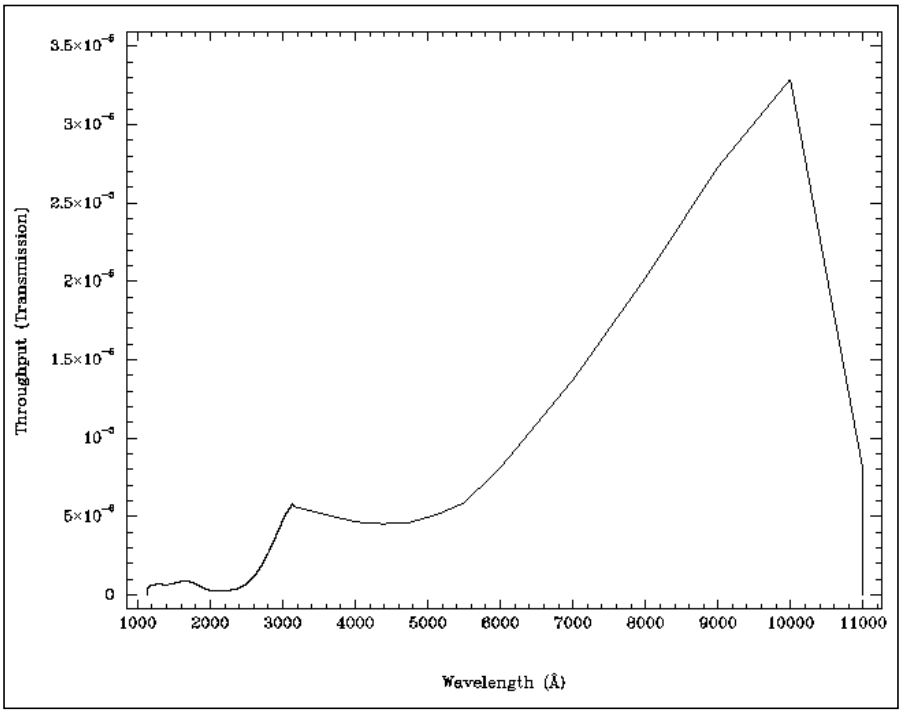

Proposal ID 8070: Throughput of CN182, CN270, MgII, CIII Filters

Execution	Executed as planned on Sept. 21-22, 1998.
Summary of Goals	Measure the absolute sensitivity of the NUV-MAMA imaging modes with the CN182, CN270, MGII, and CIII filters.
Summary of Analysis	The analysis is reported in a draft ISR (Ferguson *et al.* 1999) and is in progress (C. Proffitt). Products include the reference file j781536qo_apt, Synphot updates, and the IHB, ch. 5 (see Fig. 24). The PHOTFLAM values (e.g., as recorded in the science header) do not required an update since the measurements are consistent with those taken before the launch. For the CCD the measurements indicate a 25% drop in sensitivity for the F28X50LP aperture relative to pre-launch estimates. The physical origin of this drop has not been identified. For the 50CCD aperture, the single standard star measurement analyzed suggests a 4% drop in sensitivity. Also, there is no significant indication of a wavelength dependence. For more information refer to the STIS Quick-Look Analysis Report 7661.
Accuracy Achieved	All the STIS imaging throughputs are within 30% of the pre-launch estimates. For the FUV-MAMA imaging modes, the calibration is within 6% of the pre-launch estimates, and the various measurements agree to within 4%. For the NUV-MAMA imaging on orbit sensitivities are within 2% to 17% of pre-launch predictions.
Continuation Plans	Further measurements are required to confirm the change in sensitivity for the CCD.

Figure 24: Left: the F25MGII (MgII filter) and F25CN270 (CN270 filter) integrated system throughputs (IHB, Fig. 5.14). **Right:** the F25CIII and F25CN182 integrated system throughputs (IHB, Fig. 5.15). Sensitivities for these filters are given in the IHB, ch. 14.

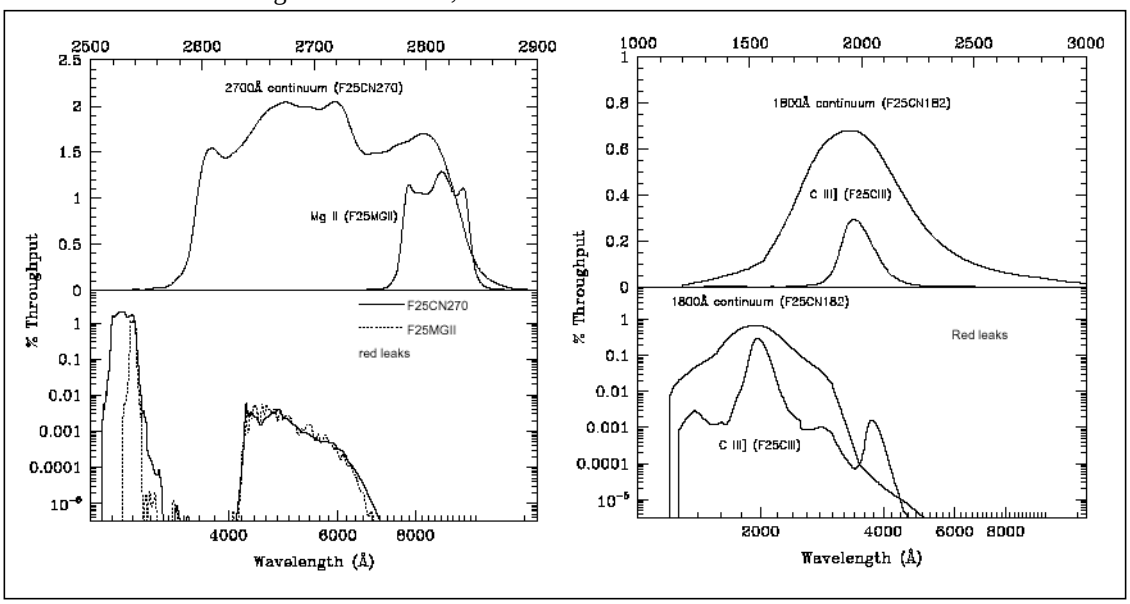

Proposal ID 8438: CCD Saturated Photometry

Execution	Executed as planned on May 14, 1999.
Summary of Goals	Explore the capability of the STIS/CCD to support high S/N time-series photometry well in excess of the S/N=10000 level expected from counting 10^8 electrons per spectrum before saturation.
Summary of Analysis	The analysis is given in the ISR 99-05 (see Table 16).
Accuracy Achieved	S/N near 10000 per read-out was demonstrated.
Continuation Plans	Not included in future calibration plans.

Table 16. Time-series signal-to-noise results for α Cen A and B observations (proposal 8438) that show a S/N greater than 9000 for α Cen A, for details and results refer to the ISR 99-05.

Case	A	B	Comment
1	843	3825	Direct extrapolation.
2	8498	5332	Exponential fit subtracted.
3	8839	6422	x, y, background regressions.
4	9444	6860	A by B, and B by A regressions.

7. Operations and Engineering

Proposal ID 7605: Target Acquisition Workout

Execution	Four different targets acquired in June and August 1997. Visits for target LDS7498 withdrawn (2 external orbits).
Summary of Goals	Test the STIS target acquisition software using the ACQ and ACQ/PEAK modes.
Summary of Analysis	The analysis is given in the TIR 99-04. Products include the IHB, ch. 8 and the online STIS Target Acquisition Simulator. For a technical description of the CCD target acquisition design refer to the TIR 96-10.
Accuracy Achieved	Point source: accurate to 0.01 arcseconds. Diffuse source: accurate within 0.01-0.1 arcseconds.
Continuation Plans	Not included in future calibration plans.

Proposal ID 7660: STIS to FGS Alignment, CCD

Execution	Executed as planned during Jan. and Feb. 1998.
Summary of Goals	Verify the transformation of the CCD detector reference frame to the FGS reference frame following a PDB update.
Summary of Analysis	The prior PDB update (Jan. 1998) was confirmed and no changes were necessary. The PDB SIAF file is available from the Observatory (OSG) web page, *http://www.stsci.edu/instruments/observatory/siaf.html*.
Accuracy Achieved	The accuracy of the aperture zero point (V2, V3) is less than or equal to 0.1 arcsec, the accuracy of the rotation angle is less than 0.5 degrees, and the CCD plate scale accuracy is approximately 0.1%.
Continuation Plans	Repeated in proposal 8503 in SMOV for SM3A.

Proposal ID 7643: MAMA Fold Distribution

Execution	Unlike the MAMA Fold Analysis proposal 7965 this proposal only executes in the case that an anomalous recovery of the NUV- or FUV-MAMA is necessary (ISR 98-03). A NUV-MAMA recovery executed in Sept. 1999. The FUV-MAMA recovery was not used in Cycle 7.
Summary of Goals	Measure the distribution of charge cloud sizes incident upon the anode during recovery procedures.
Summary of Analysis	Fold analysis draft report (Long 1999a), see Fig. 25. Procedures described in the ISR 98-02R and TIR 97-09.
Accuracy Achieved	Measurements are compared with previous results.
Continuation Plans	New standing Cycle 9 proposals are submitted with changes based on Cycle 7 experience.

Figure 25: The fold distribution (refer to the Fig. 11 caption) for day 273 shows that the NUV-MAMA has not been degraded after the recovery from a bright object violation. The Software Global Monitor event rate for the NUV-MAMA was exceeded on Sept. 18, 1999 (during the execution of proposal 6603: *Probing Proto-Planetary Disks in the Orion Nebula*). The fold analysis plot shows that there is no degradation of the MAMA micro-channel plate. Problems would appear as a deviation (greater than 20% counts per fold per event) in the distribution of a fold number. (Long 1999a)

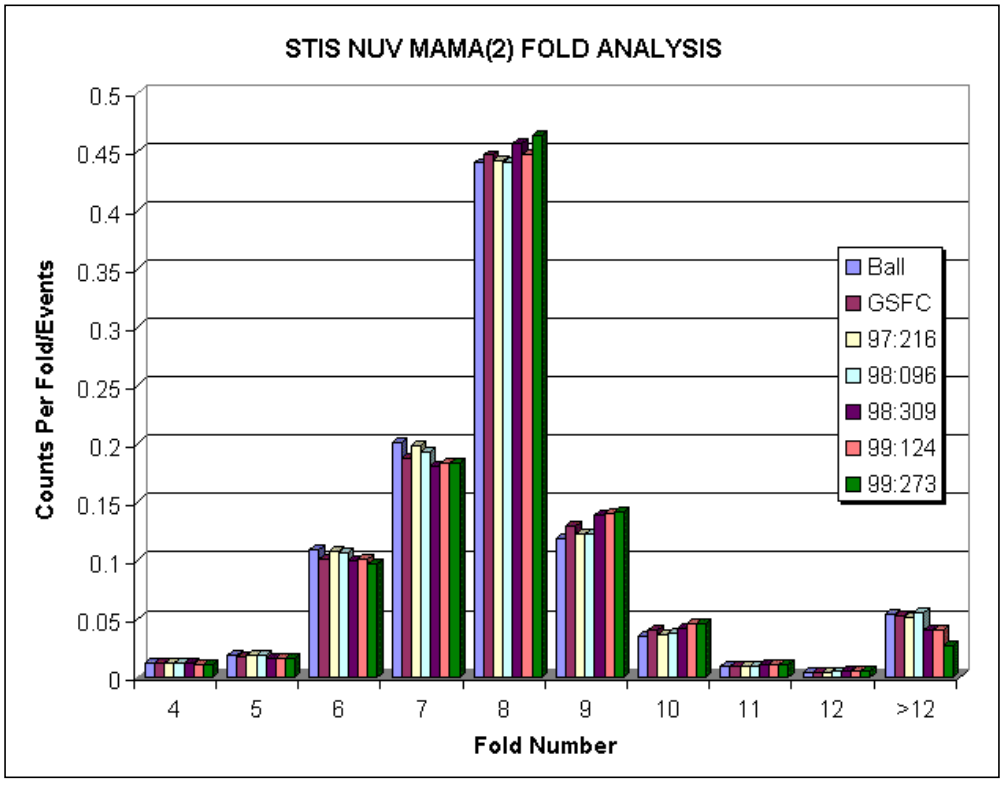

Proposal ID 7646: CCD Scattered Light from Earth Limb

Execution	Executed as planned on December 9-13, 1997.
Summary of Goals	Analyze the effect of scattered light from the bright limb of the Earth on the background of STIS CCD images
Summary of Analysis	The analysis is reported in the ISR 98-21 (see Fig. 26).
Accuracy Achieved	Background of the scattered light from the Earth limb may be measured to 0.001 e^- sec^{-1} pix^{-1}.
Continuation Plans	Excluded from future calibration plans, at this time future measurements are not necessary.

Figure 26: The CCD measurements of the scattered light from the Earth limb. **Left:** The dramatic increase in the background level with decreasing limb angle is well characterized by an exponential; a power law fit gives a background count rate:

$C_{BG}= 3.4564x10^{-0.06564\alpha}$ e^- sec^{-1} pix^{-1}, where α is the limb angle in degrees. Within 20˚ the light distribution on the images becomes spatially non-uniform at a level exceeding 1σ deviations from the read noise. **Right:** The background for the image obtained at the most extreme bright limb angle is strongest at low x- and high y-coordinates. (ISR 98-21).

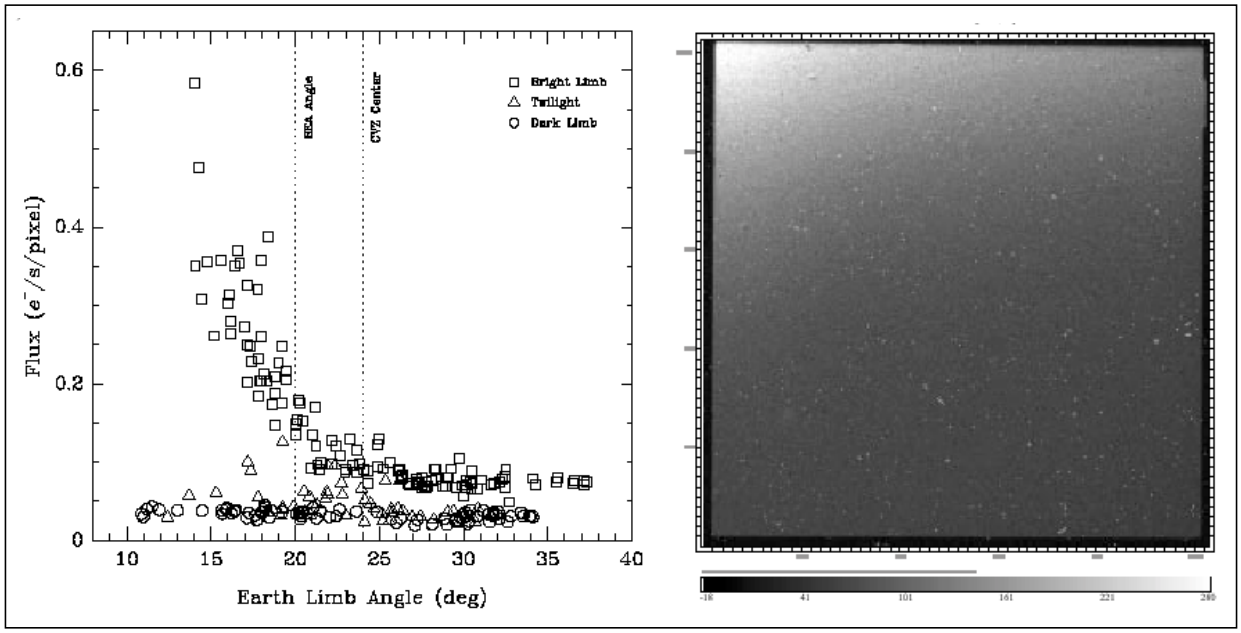

Proposal IDs 7719, 7725: FUV-, NUV-MAMA Anomalous Recovery

Execution	Linked to the execution of the fold distribution proposal 7643. The NUV-MAMA recovery executed in Sept. 1999. The FUV-MAMA recovery was not required in Cycle 7.
Summary of Goals	Permit recovery of the FUV-MAMA detector after an anomalous shutdown. Anomalous shutdowns can occur as a result of bright object violations which trigger the Bright Scene Detection or Software Global Monitors. Anomalous shutdowns can also occur as a result of MAMA hardware problems.
Summary of Analysis	The analysis is given in a draft report (Long 1999a). Procedures given in the ISRs 98-03, 96-027. The ISR 98-03 specified that the OR count rate should not exceed 7000 counts/sec for the NUV-MAMA and 10,000 counts/sec for the FUV-MAMA, however, these rates depend on the MAMA charge amplifier temperature, shown in Fig. 27, and differ from the ISR 98-03 values.
Accuracy Achieved	Not applicable.
Continuation Plans	New Cycle 9 proposals are submitted with changes based on Cycle 7 experience.

Figure 27: MAMA amplifier noise as a function of charge amplifier temperature with an amplifier threshold of 0.28 volts (noise counts courtesy of V. Argabright, Ball Aerospace).

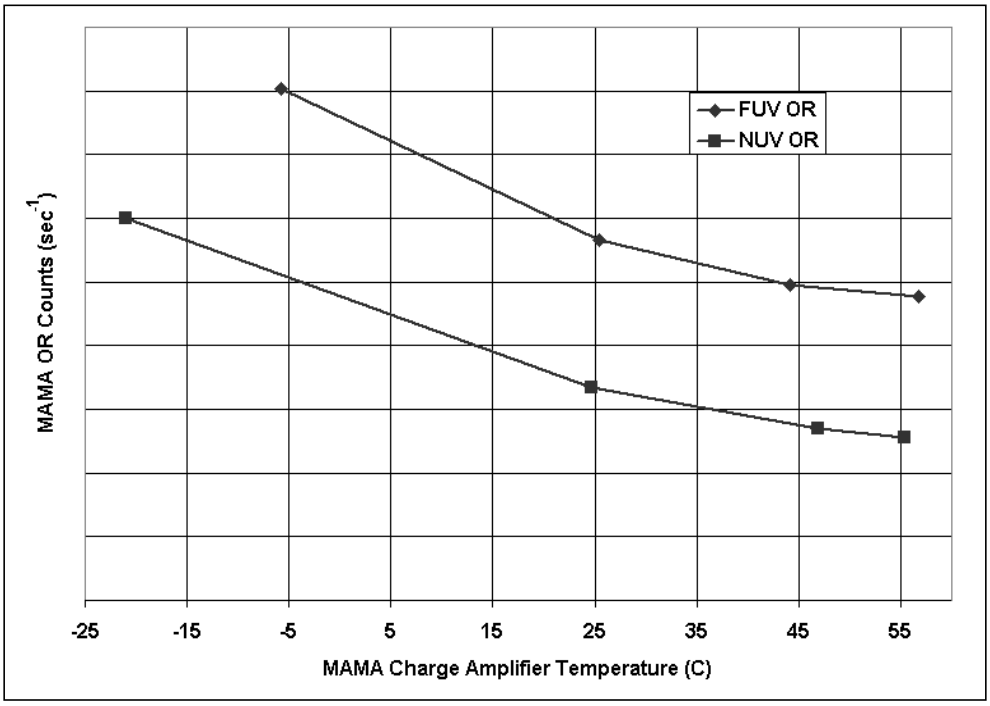

Proposal ID 7721: Slit Throughputs, MAMA

Execution	Executed as planned on Oct. 1997.
Summary of Goals	Determine the throughput versus wavelength for a variety of commonly used slits.
Summary of Analysis	The analysis is given in the ISRs 98-20 and 98-01 (including transmission versus wavelength plots). A summary of the analysis is given in Table 17. Products include reference file updates (apt).
Accuracy Achieved	Refer to Table 17.
Continuation Plans	Not included in the Cycle 8 calibration plan.

Table 17. The range of transmission over the wavelength of the adopted model, along with the 1σ scatter (*rms*) and worst case minimum and maximum range of the observed transmission with respect to the adopted model. (ISR 98-20)

Aperture	Transmission	RMS (%)	Min. (%)	Max (%)
0.1x0.09	0.36-0.69	-	-	-
0.2x0.06	0.33-0.59	-	-	-
0.2x0.09	0.40-0.69	-	-	-
0.2x0.2	0.52-0.77	5.0	-5	+10
52x0.05	0.28-0.50	11.8	-30	+3
52x0.1	0.48-0.75	8.8	-24	+8
52x0.2	0.63-0.86	4.5	-10	+10
52x0.5	0.82-0.93	2.7	-6	+6
52x2	0.96-0.99	1.3	-4	+2

Proposal ID 7722: Lamp Flux Measurement

Execution	Executed as planned during Aug. and Sept. 1997.
Summary of Goals	Determine the optimal configuration for obtaining science-contemporaneous wavecals (wavelength calibration images).
Summary of Analysis	The configurations for the wavelength calibration system are given in the TIR 98-07 (refer to Table 18). Products include a STIS Flight Software table update and the ETC update.
Accuracy Achieved	Not applicable.
Continuation Plans	Not continued during the Cycle 8 calibration.

Table 18. Cycle 7 lamp configurations (TIR 98-07). “Explicit lamp” type requires lamp specification in the Phase 2 proposal.

Lamp	Disperser	Central Wavelength (Å)	Type
HITM	G140L	1425	auto wavecal
	G140M	1222	auto wavecal
	G230M	2376	explicit lamp
	G430L	4300	explicit lamp
	G750M	6768	auto wavecal
LINE	G140L	1425	auto wavecal
	E140M	1425	explicit lamp
	E230M	2707	auto wavecal
	G230LB	2375	auto wavecal
	G230M	2419	explicit lamp
	G750M	6581	auto wavecal
TUNGSTEN	G750L	7751	explicit lamp

Proposal ID 7905: CCD Acquisition Checkout for Hot Pixel Fix

Execution	Executed as planned on Feb. 6-8, 1998.
Summary of Goals	Verify that the updated STIS Flight Software corrects for hot pixels, using a point source and a diffuse source, and that the ACQ/PEAK is not adversely affected by the FSW update.
Summary of Analysis	The tests were successfully executed and the Flight Software was immediately released for use, so that weekly hot pixel table updates were no longer necessary. If a severe hot pixel develops in the 32x32 subarray for the lamp illumination phase or a dead pixel develops, the hot pixel table may need to be updated, but for now the hot pixel table is set to *off*. An anomaly was noted during the point source ACQ dithered observation, some pixels at the 3-5 DN level persisted. But the level does not appear to scale with exposure time and should not pose a problem for acquisitions. (STIS Quick-Look Analysis Report 7905)
Accuracy Achieved	Point source (ACQ): accurate to 0.1 pixels in both AXIS1 and AXIS2 axes for dithered and undithered cases. Diffuse source (ACQ): accurate (centering of the target is hard to determine due to its diffuse nature) to 1.1 and 1.4 pixels in AXIS1 and AXIS2 respectively; these numbers are consistent with previous diffuse ACQ accuracies. Point source (ACQ/PEAKs): the imaging peak-ups (3 steps each) appeared to have worked successfully, as well as the (5 step) spectroscopic peak-up, which was accurate to 0.05 pixels (3% of the aperture size).
Continuation Plans	Not continued during the Cycle 8 calibration.

Proposal ID 7951: Anomalous Scatter Calibration

Execution	Executed as planned on July 13, 1998.
Summary of Goals	Characterize the scattered light patterns seen in the G750L and G230MB modes.
Summary of Analysis	The analysis is not complete since it is low priority and there is not enough demand for observations using the occulting bar. The analysis may be out sourced in the future. The data is sufficient for analysis and includes CCD observations using the (1) G750L mode with the 52X0.2F1 aperture, (2) G750L mode with the 52X0.2 aperture, and (3) MIRVIS mode with the F25ND3 filter.
Accuracy Achieved	Not available.
Continuation Plans	Not included in the Cycle 8 calibration plan.

Proposal ID 7953: Slit Wheel Repeatability

Execution	Executed as planned on Jan. 25, 1999.
Summary of Goals	Check the stability of the STIS slit wheel from a sequence of comparison lamp spectra using the G230M (centered at 3055 Å) mode.
Summary of Analysis	On orbit measurements are consistent with previous measurements and the distribution of positions for the slit wheel, summarized in the STIS Quick-Look Analysis Report 7953 (see Table 19 and Fig. 28). For previous results refer to the ISR 95-10.
Accuracy Achieved	Measurements have an accuracy of 0.01 pixels or 0.5 milli-arcseconds.
Continuation Plans	Cycle 8 proposal 8417, executed on Jan. 12, 2000, results included in Table 19 and Fig. 28.

Table 19. Distributions of positions from the slit wheel repeatability measurements. On orbit measurements are consistent.

Date of Measurement	Dispersion Direction (AXIS1)	Spatial Direction (AXIS2)
May 8, 1995 (Ball)	0.15 pixels (7.5 milli-arcsec)	0.05 pixels (2.5 milli-arcsec)
Jan. 25, 1999 (Cycle 7)	0.06 pixels (3.0 milli-arcsec)	0.03 pixels (1.5 milli-arcsec)
Jan. 12, 2000 (Cycle 8)	0.05 pixels (2.5 milli-arcsec)	0.03 pixels (1.5 milli-arcsec)

Figure 28: The distribution of positions for the STIS slit wheel (Cycle 8 distributions shown, very similar to Cycle 7). The Cycle 7 and Cycle 8 distributions are an improvement from the ground measurements made at Ball Aerospace (ISR 95-10), given in Table 19.

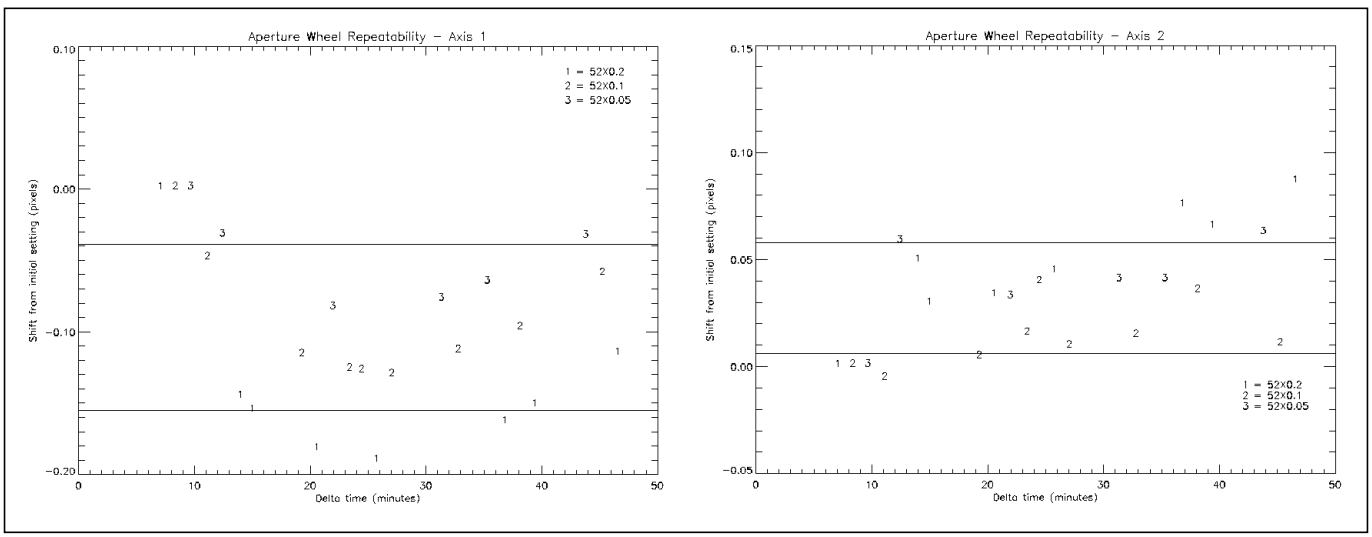

Proposal ID 8051: STIS Out-of Focus PSF

Execution	Executed in June 1998 using the standard star GRW+70D5824. 1 orbit had guiding problems.
Summary of Goals	Obtain out-of-focus images by observing standard stars with well established fluxes, using filters.
Summary of Analysis	The analysis is in progress. The data appears sufficient for analysis and includes CCD images using the F28X50OII and F28X50OIII filters, as well as, MAMA images using the F25MGII, F25CIII, and F25LYA images.
Accuracy Achieved	Not available.
Continuation Plans	Not included in the Cycle 8 calibration plan.

Proposal ID 8397: MSM Update Spectroscopic Verification

Execution	Executed as planned on Mar. 15, 1999. Replaced Proposal 7942, which was withdrawn.
Summary of Goals	Wavelength calibration images (wavecals) will be taken in the G140L and G140M modes to check the positioning of the spectrum on the detector after the MSM update. The MSM update changes the projection of spectra taken in the first-order mode so that typical observations will project the source to a location with lower dark current.
Summary of Analysis	In March 1999, the Mode Select Mechanism (MSM) was adjusted to center images better in the vertical direction. For the FUV-MAMA, the placement of first order spectra was moved about 3 arcsec. below the nominal detector center to avoid the high background in the upper-left quadrant. Subsequent observations from proposal 8397 verified the MSM and image location. The MSM positions for the G140L and M modes were also changed in July 1997, refer to the IDT Post-Launch Quick-Look Analysis Report 056.
Accuracy Achieved	The plate scale accuracy for the FUV-MAMA is 0.08% (refer to proposal 7788).
Continuation Plans	Not included in the Cycle 8 calibration plan.

8. Withdrawn or Replaced

Proposal ID 7934: Repeller Wire Off Test

Execution	All observations withdrawn, replaced by a Cycle 8 proposal.
Summary of Goals	Demonstrate that a resolving power of 220, 000 can be achieved with an external target with E140H using the high resolution mode, the 0.1x0.025 arcsec. slit and the repeller field off.
Summary of Analysis	Not applicable since observations were withdrawn due to lack of interest from the GO community during Cycle 7.
Accuracy Achieved	Not applicable since observations were withdrawn.
Continuation Plans	Cycle 8 proposal 8431, out-sourced to Ted Gull (STIS IDT).

Proposal ID 7935: Cross Disperser Mode Test

Execution	All observations withdrawn.
Summary of Goals	Test the cross-disperser mode functionality and sensitivity.
Summary of Analysis	Withdrawn since the GO community did not request the use of cross disperser modes during Cycle 7. Description of the cross disperser modes given in the TIR 97-22.
Accuracy Achieved	Not applicable since observations were withdrawn.
Continuation Plans	Not included in future Cycles.

Proposal ID 7942: MSM Update Test

Execution	All observations withdrawn, replaced with proposal 8397
Summary of Goals	Verify the position of spectra following an MSM update.
Summary of Analysis	Refer to the Cycle 7 proposal 8397.
Accuracy Achieved	Not applicable since observations were withdrawn.
Continuation Plans	Not included in future Cycles.

9. References

4. Ayres, T., *et al.* 1999, Proc. AAS, 194.6701A
5. Beck, T., Landsman, W. 1997, in *The 1997 HST Calibration Workshop*, ed. Casertano, S., Jedrzejewski, R., Keyes, T., Stevens, M., p. 165 (Baltimore: STScI)
6. Bohlin, R. 2000, AJ, 120, 437B
7. Bohlin, R., & Colina, L. 1997, AJ, 113, 1138
8. Bohlin, R., *et al.* 1990, ApJ Suppl., 73, 413
9. Dashevsky, I., Caldwell, J. 2000, Proc. AAS, 196.3211D
10. Ferguson, H., Smith, E., Walsh, J., Tolstoy, E., Plait, P. 1999, Draft ISR: *STIS Image-mode Throughputs*
11. Ferguson, H. 1998, in the October *STScI Newsletter*, p. 7 (Baltimore: STScI)
12. Ferguson, H. 1997, in *The 1997 HST Calibration Workshop*, ed. Casertano, S., Jedrzejewski, R., Keyes, T., Stevens, M., p. 90 (Baltimore: STScI)
13. Gardner, J. P., *et al.* 2000, AJ, 119, 486
14. Gilliland, R. L., *et al.* 1999, PASP, 111, 1009
15. Goudfrooij, P., 2000, in the Workshop on HST CCD Detector CTE (Baltimore: STScI)
16. Goudfrooij, P., *et al.* 1997, in *The 1997 HST Calibration Workshop*, ed. Casertano, S., Jedrzejewski, R., Keyes, T., Stevens, M., p. 100 (Baltimore: STScI)
17. Hill, R. S., *et al.* 1997, in The 1997 HST Calibration Workshop, ed. Casertano, S., Jedrzejewski, R., Keyes, T., Stevens, M., p. 120 (Baltimore: STScI)
18. Howk, J. C., Sembach, K. R. 2000, AJ, 119, 2481
19. Kaiser, M. E., *et al.* 1998, PASP, 100, 978
20. Kimble, R., *et al.* 1998, ApJ, 492L, 83
21. Kriss, J. 1999, in the December *STScI Newsletter*, p. 7 (Baltimore: STScI)
22. Landsman, W., & Bowers, C. 1997, in *The 1997 HST Calibration Workshop*, ed. Casertano, S., Jedrzejewski, R., Keyes, T., Stevens, M., p. 132 (Baltimore: STScI)
23. Leitherer, C., *et al.* 2000, STIS Instrument Handbook, Version 4 (Baltimore: STScI)
24. Long, Chris 1999a, Draft: *STIS Technical Report 99:287 Orion Nebula Surface Brightness Exceed NUV MAMA Illumination Limits*
25. Long, Chris 1999b, *STIS Engineering Update 99:195 MAMA Fold Analysis*

26. Malumuth, E. M., & Bowers, C. 1997, in *The 1997 HST Calibration Workshop*, ed. Casertano, S., Jedrzejewski, R., Keyes, T., Stevens, M., p. 144 (Baltimore: STScI)

27. Plait, P., & Bohlin, R. 1997, in *The 1997 HST Calibration Workshop*, ed. Casertano, S., Jedrzejewski, R., Keyes, T., Stevens, M., p. 150 (Baltimore: STScI)

28. Woodgate, B. E., *et al.* 1998, PASP, 110, 1138

10. Appendix A

Table 20. STIS CCD and MAMA detector performance characteristics (IHB, table 7.1, table 7.5).

Characteristic	CCD	FUV-MAMA	NUV-MAMA
Architecture	Thinned, backside illuminated	CsI photocathode	Cs_2Te photocathode
Wavelength range	2000-11000 Å	1150-1700 Å	1600-3100 Å
Pixel format	1024 x 1024	1024 x 1024	1024 x 1024
Field of view	52 x 52 arcseconds	25.1 x 25.3 arcseconds	25.1 x 25.4 arcseconds
Pixel size	21 x 21 μm	25 x 25 μm	25 x 25 μm
Pixel plate scale	0.05071 arcseconds	0.0245 x 0.0247 arcseconds	0.0245 x 0.0248 arcseconds
Quantum efficiency	~20% @ 3000 Å ~67% @ 6000 Å ~29% @ 9000 Å	25% @ 1216 Å	10% @ 2537 Å
Dark count	0.003 e^- sec^{-1} pix^{-1} @ -83 C	$5x10^{-6}$ to 10^{-5} counts sec^{-1} pix^{-1}	$8x10^{-4}$ to $1.7x10^{-3}$ counts $sec.^{-1}$ pix^{-1}
Global count-rate		285000 counts $sec.^{-1}$	285000 counts $sec.^{-1}$
Local count-rate		~220 counts $sec.^{-1}$ pix^{-1}	~340 counts $sec.^{-1}$ pix^{-1}
Read noise (effective values)	4.0 e^- arms at gain=1 7.7 e^- arms at gain=4		
Full well: inner portion of detector	144000 e^-		
Full well: outer portion of detector	120000 e^-		
Saturation limit	33000 e^- at gain=1 144000 e^- at gain=4		

Figure 29: Orientation of the STIS detectors with respect to the HST Vehicle and User reference frames.

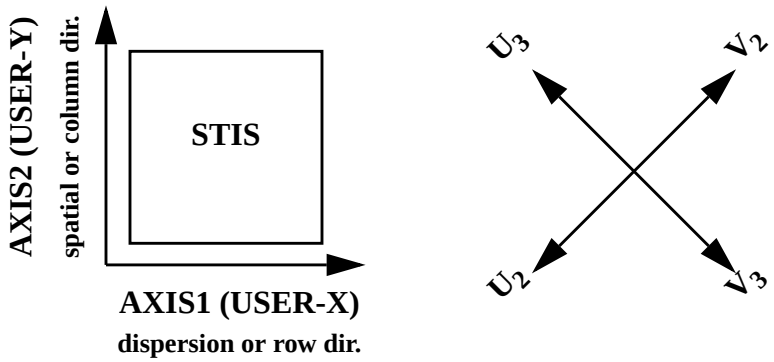

11. Appendix B

Calibration reference files for the STIS detectors are described in ICD47 and listed online at the HST Spectrographs web site:

http://www.stsci.edu/instruments/stis

Table 21. STIS CCD and MAMA calibration reference files.

File Description	Suffix	Type	Detector
Bias image file.	bia	image	CCD
Dark image file.	drk	image	CCD & MAMAs
Pixel-to-pixel flat image file.	pfl	image	CCD & MAMAs
Delta flat image file.	dfl	image	CCD & MAMAs
Low-order flat image file.	lfl	image	CCD & MAMAs
Shutter shading correction image file.	ssc	image	Not Available
Small scale distortion image file.	ssd	image	Not Available
Bad pixel table.	bpx	binary table	CCD & MAMAs
CCD parameters table.	ccd	binary table	CCD
MAMA linearity table.	lin	binary table	MAMAs
Analog-to-digital conversion table.	a2d	binary table	Not Available
Photometric conversion table.	pht	binary table	CCD & MAMAs
Aperture throughput table.	apt	binary table	CCD & MAMAs
Calibration lamp table.	lmp	binary table	CCD & MAMAs
Aperture description table.	apd	binary table	CCD & MAMAs
Image distortion correction table.	idc	binary table	Not Available
Two dimension spectrum distortion correction.	sdc	binary table	CCD & MAMAs
Incidence angle correction table.	iac	binary table	CCD & MAMAs
Dispersion coefficients table.	dsp	binary table	CCD & MAMAs
One dimensional spectrum trace table.	1dt	binary table	CCD & MAMAs
One dimensional extraction parameters table.	1dx	binary table	CCD & MAMAs
MAMA offset correction table.	moc	binary table	MAMA
Cosmic ray rejection parameters table.	crr	binary table	CCD
Photometric correctin table.	pct	binary table	CCD & MAMAs
Wavecal parameters table.	wcp	binary table	CCD & MAMAs

12. Appendix C: STIS ISRs, TIRs, and IDT Analysis Reports

Table 22. STIS Instrument Science Reports (ISRs) following launch in 1997. The complete list, including reports from 1995 - 1997, of ISRs is available online from the Spectrographs website: *www.stsci.edu/instruments/stis*.

Number	Title	Author(s)	Date
2000-01	Revised Bright Object Protection Policies for MAMA Observations	G. Kriss	03/14/00
99-08	Creation and Testing Procedures for STIS CCD Bias Reference Files	P. Goudfrooij	11/30/99
99-07	Changes in Sensitivity of the Low Dispersion Modes	R. Bohlin	11/24/99
99-06	Flat Fields for the CCD Spectral Modes	R. Bohlin	09/24/99
99-05	STIS/CCD Time Series Photometry with Saturated Data	R. Gilliland	08/05/99
99-04	Dust Motes and Blemishes in the CCD Spectral Modes	R. Bohlin	07/26/99
99-03	Calsits 6: Extraction of 1_D Spectra in the STIS Calibration Pipeline	M. McGrath, I. Busko, P. Hodge	04/02/99
99-02	Scientific Requirements for Thermal Control and Scheduling of the STIS MAMA Detectors after SM-3	H. Ferguson, S. Baum	03/07/99
99-01	Internal to External Wavelength Calibration	K. Sahu	02/15/99
98-31	STIS CCD Performance Monitor: Read Noise, Gain, and Consistency of Bias Correction during June 1997 - June 1998	P. Goudfrooij	11/15/98
98-30	Specification and Application of the MAMA Additive Image (MADDIM) to Track Charge Extraction	J. Walsh, S. Baum, J. Rose, J. Hayes	02/01/98
98-29	STIS Near-IR Fringing III. A Tutorial on the use of the IRAF Tasks	P. Goudfrooij, J. Christensen	11/30/98
98-28	The STIS Pipeline - Determination of Calbration Switch Settings	R. Downes	10/20/98
98-27	Sensitivity Monitor Report for the STIS First-Order Modes	N. Walborn, R. Bohlin	10/12/98
98-26	Calstis 1: Basic Two-Dimension Image Reduction	P. Hodge, S. Baum, P. Goudfroij	10/12/98
98-25	Echelle Neutral Density Slit Throughputs	C. Leitherer, R. Bohlin, P. Plait	10/22/98
98-24	Spectroscopic Mode Peculiarities	C. Bowers, S. Baum	06/11/98
98-23	Plate Scales, Anamorphic Magnification and Dispersion: CCD Modes	C. Bowers, S. Baum	07/14/98
98-22	Cosmic Ray Rejection in STIS CCD Images	R. Shaw, P. Hodge	06/19/98

Number	Title	Author(s)	Date
98-21	Scattered Light from the Earth Limb Measured with the STIS CCD	R. Shaw, M. Reinhart, J. Wilson	06/17/98
98-20	Clear Aperture Fractional Transmission for Point Sources	R. Bohlin, G. Hartig	10/12/98
98-19	STIS Near-IR Fringing II. Basics and Use of Contemporaneous Flats for Spectroscopy of Point Sources (Revision A)	P. Goudfrooij, R. Bohlin, J. Walsh, S. Baum	11/22/98
98-18	Absolute Flux Calibration for Prime STIS Echelle Modes with the 0.2”X0.2” Slit	R. Bohlin	06/01/98
98-16	Use of FP-SPLIT Slits for Reaching High Signal-to-Noise with MAMA Detectors	R. Gilliland	04/09/98
98-15	MAMA Flat-Field Status and Plans	R. Shaw, M. Kaiser, H. Ferguson	04/06/98
98-14	The Calstis IRAF Calibrtion Tools for STIS Data	R. Katsanis, M. McGrath, STIS Pipeline Block	04/26/98
98-13	Calstis7: Two-dimensional Rectification of Spectroscopic Data in the STIS Calibration Pipeline	M. McGrath, P. Hodge, S. Baum	05/05/98
98-12	Calstis4, Calstis11, Calstis12: Wavecal Processing in the STIS Calibration Pipeline	P. Hodge, S. Baum, M. McGrath, S. Hulbert, J. Christensen	04/22/98
98-11	Calstis2: Cosmic Ray Rejection in the STIS Calibration Pipeline	R. Shaw, J. Hsu, STIS Pipeline Block	05/04/98
98-10	Calstis0: Pipeline Calibration of STIS Data - A Detailed View	P. Hodge, S. Baum, M. McGrath, R. Shaw	04/22/98
98-09	Extraction Heights for STIS Echelle Spectra	C. Leitherer, R. Bohlin	04/15/98
98-08	MAMA Bright Object Checking: Experience from Cycle 7 and Recommendations for Cycle 8	C. Leitherer	04/01/98
98-06	STIS CCD Anneals	J. Hayes	03/01/98
98-05	Doppler Compensation in CALSTIS	K. Sahu, P. Hodge, S. Kraemer	02/01/98
98-04	Spectroscopic Mode Image Quality of STIS I. First Order Modes	K. Sahu, S. Hulbert, H. Lanning, J. Christensen	01/30/98
98-03	MAMA Anomalous Recovery	H. Ferguson, M. Clampin, S. Kraemer, V. Argabright	10/22/98
98-02	Cycle 7- MAMA Pulse Height Distribution Stability: Fold Analysis Measurement (Revision A)	H. Ferguson, M. Clampin, V. Argabright	10/22/98
98-01	Diffuse Source Absolute Sensitivity and Point Source Relative Sensitivity as a Function of Extraction Slit Height for STIS First-Order Modes	R. Bohlin	02/01/98

Number	Title	Author(s)	Date
97-16	STIS Near-IR Fringing: Basics and Use of Contemporaneous Flats for Extended Sources	S. Baum	12/01/97
97-15	GO Added Near-IR Flats (Revision A)	S. Baum, H. Ferguson, J. Walsh, P. Goudfrooij, R. Downes, H. Lanning	12/01/97
97-14	Absolute Flux Calibration for STIS First-Order Low-Resolution Modes	R. Bohlin	12/01/97
97-13	Extraction Slits for First-Order STIS Spectra	C. Leitherer	09/01/97
97-12	STIS Target Acquistions During SMOV	R. Katsanis	07/01/97
97-11	STIS Paper Products (Revision A)	S. Keener	05/01/97
97-10	STIS Results from SMOV: CCD Baseline Performance	P. Goudfrooij	05/01/97
97-09	The STScI STIS Pipeline: Bias Level Correction	P. Goudfrooij	05/01/97
97-08	The Spectrum Splicer Task	S. Hulbert	05/01/97
97-07	Pre-Launch NUV MAMA Flats	R. Bohlin	05/01/97
97-06	Mode Selection Mechanism Repeatability	R. Downes	04/01/97
97-05	The STSci STIS Pipeline IV: Combining REPEAT-OBS Data (Revision A)	P. Goudfrooij	03/01/97
97-03	A User's Guide to Target Acquisition with STIS (Revision B)	R. Downes	05/01/97
97-02	The STScI STIS Pipeline VII: Extraction of 1-D Spectra	S. Hulbert	02/01/97
97-01	Automatic and GO Wavecals for CCD and MAMA Spectroscopic Observations	S. Baum	02/01/97

Table 23. STIS Technical Instrument Reports (TIRs) following launch. A complete list is available from the STIS Internal website at *www.stsci.edu/internal/stis* (access may be prohibited for users not employed at STScI).

Number	Title	Author(s)	Date
2000-03	STIS Moving Target Long-Range Plan	Alex Storrs	05/19/00
2000-02	STIS Testing for On-The-Fly Calibration (OTFC) Systems	G. Mitchell, M. McGrath	04/20/00
2000-01	The STIS Reference File Checking Tool	R. Downes, R. Miller	04/11/00
99-04	Forensics: How to Autopsy a Target Acquistion	R. Downes	07/13/99
99-03	Revised Dispersion Solution Software	B. Espey	05/26/99

Number	Title	Author(s)	Date
99-02	STIS Coordinate System Orientation and Transformations	G. Hartig, E. Kinney, P. Hodge, M. Lallo, R. Downes	02/15/99
99-01	STIS Cycle 8 GO Contact Scientist Review Procedure	C. Leitherer	01/29/99
98-13	The Spectrographs Group Internal Help Desk Procedure	J. Wilson, R. Downes, J. Christensen, A. Gonnella, E. Smith, H. Lanning	12/03/98
98-12	Assessment and Delivery of Spectrographs Calibration Reference Files	J. Christensen, R. Downes, M. McGrath	08/10/98
98-11	Interim Spectrographs Group Plan 6/98	S. Baum, Spectrographs Group	07/14/98
98-10	STIS MAMA High and Low Voltage Management Around the SAA	S. Baum, M. Reinhart, and H. Ferguson	07/07/98
98-09	Delivering STIS Synphot Component Files	J. Wilson, E. Kinney	04/21/98
98-08	MAMA Bright Object Protection Procedures for Solar System Observations	M. McGrath	04/08/98
98-07R	The STIS Monthly Monitoring Program	R. Downes, A. Gonnella, R. Katsanis	06/28/00
98-06	Scientific Benefits of a Low NUV-MAMA Dark Rate	H. Ferguson and S. Baum	02/23/98
98-05	Creation Tools for CCD Darks	J. Christensen and P. Goudfrooij	03/11/98
98-04	Synphot Component Files for STIS	E. Kinney, J. Wilson, K. Sahu, B. Simon, H. Ferguson, J. Christensen	09/17/98
98-03	Implementation Plan for an Emission Line Tool in the Spectroscopic ETC	K. Sahu, J. Wilson	01/03/98
98-02	The STIS Target Acquisition ETC	J. Wilson, K. Sahu	01/25/98
97-22	STIS Cross Disperser Modes	K. Sahu	11/17/97
97-21	A Discussion Document; Options for Cycle 8 and 9 STIS Development Activities	S. Baum, H. Ferguson, R. Downes, H. Lanning, K. Sahu	11/07/97
97-20	STIS (Spectrographs) Group Plan 9/97 Through 9/98	S. Baum, Spectrographs Group	11/14/97
97-19	Post-Observation Support Plan for the Spectrographs Group	R. Downes, J. Christensen	02/05/98
97-18	STIS ETC Training Manual: details of the file structures and description code	K. Sahu, E. Kinney	09/16/97

Number	Title	Author(s)	Date
97-17	Science Impacts of STIS Thermal Modes	S. Baum, H. Ferguson, B. Woodgate, R. Kimbl	10/16/97
97-16	STIS Flatfielding technical requirements - Revision A	H. Ferguson and S. Baum	07/22/97
97-15	STIS Absolute Photometric Calibration: Suggested Flat Field and Fringing Removal for G750L	R. Bohlin	07/01/97
97-14A	Requirements for Near-IR GO Fringe Flats - Revision A	S. Baum, H. Ferguson, and P. Goudfrooij;	07/23/97
97-13	STIS Target Acquisition Data and Analysis Plans	R. Downes, R. Katsanis, G. Hartig	07/03/97
97-12	Philosophy and Upper Limits to the Height of the Artificial Extraction Slits	R. Bohlin, G. Hartig	06/01/97
97-11	Closure of Actions Items resulting from the BOP Review of 7 January 1997	C. Leitherer, M. Clampin, S. Baum	05/01/97
97-10	An Internal Cookbook for STIS Data	A. Gonnella, J. Christensen, M. McGrath, J. Hayes, P. Hodge, R. Katsanis	05/05/97
97-09	MAMA Pulse height distribution stability: Fold Analysis Measurement	M. Clampin, V. Argabright	04/30/97
97-08	Planning for STIS Cycle 7 Calibration	M. McGrath, H. Ferguson, S. Baum	04/16/97
97-05	MAMA High Voltage Turn-on for SMOV	M. Clampin, M. Hinds, G. Hartig, S. Kraemer, V. Argabright, V. Balzano, S. Keener, S. Baum	04/21/97
97-04	STIS Pipeline Testing IV: Cosmic Ray Rejection	R. Shaw, R. Katsanis, M. Potter	03/20/97
97-03	STIS SMOV Hardware Policies	J. Hayes, E. Kinney	02/25/97
97-02	Assessment and Delivery of STIS Calibration Reference Files	M. McGrath, R. Katsanis	03/12/97
97-01	Progressive Commissioning of Cycle 7 Science through SMOV	S. Baum, H. Ferguson, S. Kraemer	02/23/97

Table 24. STIS Instrument Definition Team (IDT) Post-Launch Quick-Look Analysis Reports, available online *hires.gsfc.nasa.gov/stis/reports/reports_table.html*. These include reports for the analysis of SMOV proposals following the SM2.

Number	Title	Author	Date
063	Geometry and Approximate Correction of STIS CCD Window Ghosts	R. Hill	05/12/00
062	Echelle Wavelength Calibration Update	D. Lindler	09/23/99
061	Longslit Angles Measured in the CCD Camera Mode	D. Lindler	08/12/99
060	What is the best exposure time in presence of cosmic rays?	A. Smette	02/04/99
059	Recent Updates to CALSTIS and Echelle Scattered Light Correction	D. Lindler	02/11/99
058	Notes on the STIS CCD superdarks and superbias (DRAFT)	W. Landsman	10/29/98
057	Characteristics of the FUV-MAMA Dark Rate	W. Landsman	08/31/98
056	New MSM Positions for Modes 1.1 (G140L) and 1.2 (G140M)	R.S. Hill	07/31/98
055	Plate Scales: Band 1, Primary Long Slit Modes (Draft)	C. Bowers	07/29/98
054	Low-Frequency Flat fields for the STIS MAMAs	T. Brown	07/24/98
053	Spectrum Traces for a Subset of First-order STIS Modes	R.S. Hill	06/01/98
052	STIS Parallel Data Reduction Note: Image and Slitless Spectrum Alignment	N. Collins	06/02/98
051	Plate Scales, Anamorphic Magnification & Disp.: CCD Modes	C. Bowers	05/11/98
050	Locations of Ghosts of Bright Stars on STIS CCD Images	R.S. Hill	01/14/98
049	MAMA Contamination Monitor (SMOV 7064 and 7673)	P. Plait	10/09/97
048	STIS Signal to Noise Achievable Without Flat Fielding Your Data	D. Lindler	08/07/97
047	STIS Calibration Subsystem	M. Kaiser	09/03/97
046	Observed CCD Cosmic Ray Rates	W. Landsman	08/28/97
045	SMOV Report: Thermal Drifts in STIS	R. Robinson	08/26/97
044	SMOV Report: Examining the STIS Point Spread Function	R. Robinson	08/26/97
043	STIS CCD Image Mode Sensitivity	W. Landsman	08/22/97
042	SMOV 7104 Doppler Compensation Test Results	D. Lindler	08/22/97
041	STIS FUV-MAMA Geometric Distortion	E. Malumuth	08/06/97
040	Thermal Motion from G230MB Wavecals in SMOV 7087, Visit 2	R. S. Hill	08/01/97
039	Test of New MSM Positions: SMOV 7084, Visit 2	R. S. Hill	07/22/97
038	MAMA Image Mode Sensitivity: F25LYA, F25CIII, and F25MgII	W. Landsman	07/16/97

Number	Title	Author	Date
037	Temperature/Time Modeling of MAMA2 Phosphorescent Dark Rate	R. Kimble	07/01/97
036	STIS MAMA Spectroscopic Mode Image Quality Results	T. Beck	07/09/97
035	MAMA Sensitivity Curves for Low Resolution 1st Order Modes	N. Collins	07/02/97
034	SMOV 7100: SMOV Slit Transmission - CCD Modes	P. Plait	06/27/97
033	STIS CCD Geometric Distortion	E. Malumuth	06/23/97
032	CCD Sensitivity Curves for Low Resolution 1st Order Modes (SMOV 7094)	N. Collins	06/19/97
031	Creating STIS Calibration Darks and Hot Pixel Tables	W. Landsman	06/16/97
030	New MSM Positions from SMOV	R.S. Hill	06/06/97
029	Echelle Ripple Function for Mode 2.3 (E230M)	S. Heap	06/02/97
028	Proposal 7080 - MAMA Camera Image Quality	R. Robinson	05/29/97
027	STIS CCD Hot-pixel Annealing Results	T. Beck	05/20/97
026	Fringing and Flat Fields: Building a Better Flat	P. Plait	05/13/97
025	Check of MAMA Krypton-Lamp Optical Formats	R.S. Hill	05/08/97
024	Evolution of CCD Histograms - Post Launch	T. Beck	05/06/97
023	F28x50OIII and F28x50OII ([OIII] and [OII]) Filters Red Leak	P. Plait	05/01/97
022	Wavelength Dependency of FWHM for the STIS CCD	T. Beck	04/30/97
021	SMOV 7063: Contamination Monitor (continued)	P. Plait	04/24/97
020	STIS Diffuse Source Target Acquisition - First Execution (7068)	M. Crenshaw	04/21/97
019	STIS Point-Source Target Acquisition - Final Results (7067)	M. Crenshaw	04/16/97
018	Comparison of Observed Count Rates for GD153 as Part of SMOV 7063: Part II	P. Plait	04/09/97
017	Comparison of Observed Count Rates for GD153 as Part of SMOV 7063	P. Plait	04/01/97
016	Filter Red Leaks in F25CN182, F25CN270, F25LYA and F25CIII	P. Plait	03/31/97
015	STIS Point-Source Target Acquisition - First Execution (7067)	M. Crenshaw	03/31/97
014	The Growth Rate of STIS CCD Hot Pixels	E. Malumuth	03/26/97
013	Target Acquisition with STIS: Tips and Examples (Draft)	R. Robinson	03/26/97
012	Comparison of Observed Count Rates for G191B2B as Part of SMOV 7063	P. Plait	03/26/97
011	SMOV 7077: Spectroscopic Mode Image Quality- CCD	P. Plait	03/18/97

Number	Title	Author	Date
010	Comparison of Observed Count Rates for G191B2B as Part of SMOV 7063	P. Plait	03/17/97
009	SMOV 7083: CCD Optical Format Verification	S. Hulbert	03/17/97
008	F25MGII Filter Red Leak	P. Plait	03/17/97
007	STIS CCD Flat Fields In Orbit - A First Look (SMOV 7099)	M. Crenshaw	03/14/97
006	STIS CCD Bad Pixel Table for Target Acquisitions	T. Beck	03/13/97
005	Predicted Versus Observed Count Rates for G191B2B as Part of SMOV 7063	P. Plait	03/13/97
004	CCD Plate Scale (SMOV Test 7065)	W. Landsman	03/12/97
003	STIS CCD Optical Format Check (SMOV 7083)	R. S. Hill	03/10/97
002	Proposal 7061 - STIS CCD Functional Test	T. Beck	03/07/97
001	STIS CCD Cosmic Ray Hits Versus Orbital Position	D. Lindler	03/07/97